

Dr. Jessica Volz
Alfred Wegener Institute
Helmholtz Centre for Polar
and Marine Research
Am Handelshafen 12
27570 Bremerhaven
Germany
Jessica.Volz@awi.de

Prof. Dr. Jack Middelburg
Associated Editor *Biogeoosciences*
Utrecht University, Faculty of Geosciences
Princetonplein 9
3584 CD Utrecht
Netherlands

18 December 2019

Dear Prof. Dr. Jack Middelburg,

My co-authors and I are pleased to re-submit our original research article entitled “Impact of small-scale disturbances on geochemical conditions, biogeochemical processes and element fluxes in surface sediments of the eastern Clarion-Clipperton Zone, Pacific Ocean” for consideration in the special issue “Assessing environmental impacts of deep-sea mining – revisiting decade-old benthic disturbances in Pacific nodule areas” to *Biogeoosciences*.

We feel confident that the revisions of the two reviewers improved the quality and impact of our manuscript. We have addressed all comments carefully in the final author responses below.

Thank you for your time and consideration. If you have any questions, please do not hesitate to contact me and I will do my utmost to provide any further information that you require.

Yours sincerely,

Jessica Volz

Jessica Volz

Final author responses

Referee #1

The work constitutes one of the first of its kind, documenting the sedimentary biogeochemical impact of simulated disturbances that are likely to arise from deep-sea mining. Overall the study is very well designed, scientifically sound and well executed. The report is well written and contributes to an international framework of projects dealing with the deep-sea impacts of mining. Looking from a purely scientific/geochemical angle, the results are not surprising from a sediment diagenesis point of view, but I find it very important that the early diagenetic framework is able to explain and guide (to some extent) these type of impact assessments.

There is a couple, relatively moderate shortcomings which can be addressed in the final version:
- It would be great to see more of the undisturbed/baseline sediment geochemical profiles. I understand there will be a companion manuscript on this, but reproducing more of those results here maybe can be possible. Especially undisturbed OPD – TOC profiles would be interesting to see in this paper as well.

Author's response: We understand the referee's objection. However, we would like to point out that in fact we are showing undisturbed/baseline data (published in Volz et al., 2018, DSR I) in the present manuscript:

In figure 4, TOC contents are shown for undisturbed reference surface sediments for the different study sites, which are taken from Volz et al., 2018, DSR I (as stated in the figure caption for figure 4). Furthermore, TOC contents as well as ex-situ oxygen, nitrate and dissolved manganese concentrations for undisturbed deep sediments are shown in figure 5, which are used as baseline input for the transport-reaction model of the benthic disturbances. As this seems not to be clearly described in the present manuscript, we have adapted the methods section in Chapter 2.4 about the geochemical model setup and reaction network as following:

“We have applied a transient transport-reaction model for the sites in the BGR-RA and IOM areas (Table 1). These sites were chosen due to distinctively different sedimentation rates and OPD (Table 2). We have adapted the code of the steady state transport-reaction model, which was originally presented by Volz et al. (2018) and used pore-water oxygen, NO₃⁻, Mn²⁺ and NH⁴⁺ data as well as TOC contents of GC sediment cores from the same study as undisturbed reference data (Table 1; Table 2). Thus, the model parameters and baseline input data used for the transient transport-reaction model are the same as presented in the study by Volz et al. (2018).”

Furthermore, we have added a sentence in the caption of figure 5 that the analytical data shown in the graph represents the undisturbed/baseline data as following:

“Figure 5: Model results of the transient transport-reaction model for (a) the EBS disturbance in the German BGR-RA area and (b) the IOM-BIE disturbance in the eastern European IOM area. The model is adapted after the steady state transport-reaction model presented in Volz et al. (2018) and shows the response of the geochemical system in the sediments if steady state conditions are disturbed by the removal of the upper 10 cm (BGR-RA, average disturbance depth of BGR-PA and BGR-RA; cf. Table 3) and 7 cm (IOM; Table 3) of the sediments while maintaining the same boundary conditions but with reduced bioturbation over the first 100 years after the disturbance.”

- I find the discussion very substantial and objective. However I was wondering if more input to policy/blue economy can be given with a few more sentences. As it stands the message is that the uppermost organic-rich part is removed and a lot more oxygen seeps into the sediment. What will the policy side make of this, may sounds like a positive result? What is really the

impact here? The fact that the system comes back to original steady state is one thing, but deep-seafloor can be disturbed naturally, through different means.

Author's response: Deeper OPD means lower flux of reduced substances (NH₄, Mn etc) to the seafloor and more CO₂ production from POC degradation (i.e. lower pH) but from our current knowledge it is difficult to quantify this impact due to changed biogeochemical fluxes and also if this impact is good or bad. It will certainly change the microbial community structure and possibly meio/macro/megafauna communities. It is also difficult to assess at the moment whether this change may trigger a tipping point in combination with natural changes that are ongoing (e.g., bottom water warming, acidification, changes of carbon flux to the seafloor etc).

Therefore, based on our current knowledge, we can't give further advices for policy/blue economy. However, based on our current knowledge and in combination with ongoing natural environmental changes (e.g., bottom water warming, acidification, changes in the POC flux to the seafloor), it is difficult to assess whether the surface sediment removal may trigger a tipping point for deep-sea ecosystems." in lines 560-563.

Several line-by-line suggestions:

L46 and many more places: Please consider the repeated use of (re)equilibration of the study system. Rather than chemical equilibrium, I think what is meant here the system becomes steady-state over the course of the study's simulation timelines.

Author's response: We have replaced "re-equilibration/equilibrium" by "the system will return to (new) steady state geochemical conditions" accordingly.

L115 A more specific verb can replace 'influencing' here, maybe 'increasing'?

Author's response: We have replaced "influencing" by "increasing" accordingly.

L396 This can be confusing if not elaborated a little more, as it rapidly switches the discussion to glacial-timescales. First, how sure are we on the lower bottom O₂ levels in the LGM, when the seawater was somewhat colder with increasing mixing? If O₂ was still lower, I do not think it would be to a hypoxic extent that it is going to compress all the redox zones. But then how Mn delivery to LGM deep waters, given Mn was is the tracer used in this study? Please elaborate or I would recommend removal of this sentence.

Author's response: We have elaborated more on this (see paragraph below) as the occurrence of the solid-phase Mn maximum in surface sediments throughout the CCZ is important regarding the use of solid-phase Mn contents/depth profiles as a tracer for the removal of sediment/disturbance depth during the small-scale disturbance experiments, and thus, potential future mining-related activities. We have studied and intensively discussed the diagenetic formation of solid-phase Mn peaks as a result of lower glacial oxygen concentrations in the cited paper Volz et al., in press, EPSL. It also presents all relevant studies regarding the mechanisms and indications for lower oxygen concentrations in the glacial deep Pacific Ocean.

The paragraph has been adjusted as following:

"Volz et al. (in press, EPSL) have suggested that the widely observed solid-phase Mn enrichments in CCZ surface sediments formed in association with a more compressed oxic zone, which may have prevailed as a result of lower bottom-water oxygen concentrations during the last glacial period than today. Strong indication for lower glacial bottom-water oxygen concentrations throughout the eastern Pacific Ocean have been provided by a number of independent proxies (e.g., Anderson et al., 2019 and references therein). As a consequence of the condensed oxic zone, upward diffusing pore-water Mn²⁺ may have precipitated as authigenic Mn(IV) at a shallow oxic-suboxic redox boundary in the upper few centimeters of the sediments. After the last glacial period, the authigenic Mn(IV) peak was continuously mixed into subsequently deposited sediments by bioturbation causing

the observed broad solid-phase Mn(IV) enrichment in the surface sediments (Fig. 4; Volz et al., in press, EPSL)."

Figure 8 - the timescale is missing, was this deliberately omitted?

Author's response: The timescale has been added to the figure.

Referee #2

This manuscript is embedded within in a set of recent scientific investigations and cruises dedicated to elucidate the environmental impact of polymetallic nodule recovery from the seabed in the Clarion-Clipperton Zone (CCZ). New data (pore water and solid phase) are presented from deep seafloor tracks affected by deliberate disturbance (e.g. benthic sledges), and these are compared to data from undisturbed reference sites (which are unfortunately presented elsewhere). To investigate the long-term effect of disturbance, the data are supplemented with reactive transport modelling. The manuscript is generally well prepared, and uses a clear language. The manuscript clearly adds an original contribution to the existing literature regarding the CCZ, and puts the current work into perspective with appropriate referencing to previous work. However some important problems and shortcomings need to be resolved.

Major comments

[1] The approach to determine the disturbance depth (Section 2.3) is highly unclear. In my guess, the authors use a shifting window approach, whereby the depth profile of the disturbed site is shifted down compared to the reference site. Starting from a zero shift, the shift is gradually increased. At each shift, the Pearson correlation coefficient r is calculated. Somehow the best fit is determined (but is not explained how this is done – maximum r value?). Given that this method sustains one of the important conclusions (solid phase Mn can be used as to determine the disturbance/removal depth), I would expect more details on how it actually is done and its robustness. A figure of how the Pearson correlation coefficient varies as a function of the shifting depth seems to be a critical inclusion.

Author's response: In lines 243-245, we explain that “the highest positive linear correlations of solid-phase Mn contents ($r_{Mn} \sim 1$) between the disturbed sites and the respective undisturbed reference sites (Table 1) were used to determine the depths of the disturbances.” Thus, the maximum r value is used.

The robustness of the disturbance depth determined with the Pearson correlation using solid-phase Mn contents is verified by applying the same correlation/disturbance depth on the TOC contents as described in lines 245-248. As this correlation of the TOC contents yields to Pearson correlation coefficients between 0.73 and 0.91, the estimates for the disturbance depth based on the correlation using solid-phase Mn contents may be supported as written in lines 334-337.

[2] The optimal shifting window approach is now derived only from the Mn profile, and then verified with the TOC and porosity profiles. What if one combines the data from Mn, Toc and porosity profiles to obtain a weighted optimum to determine the “best disturbance depth”. Would this provide a more reliable measure?

Author's response: The idea of primarily using solid-phase Mn contents as a tracer for sediment removal is that it could be used during the monitoring of industrial-scale mining activities in the area of the CCZ (as pointed out in lines 558-560). We do not see how a combination of solid-phase Mn contents and TOC contents would obtain better estimates for the disturbance depth as we are already applying the correlation on both parameters. Furthermore, we do not feel that a disturbance depth could be derived from the correlation of porosity as the data does not show any variation over depth (see figure 4).

[3] Replication is fundamental to proper scientific investigation. The current analysis lacks such replication. The comparison of Mn and TOC profiles appears to be based on the comparison of a single core within the disturbed track compared to a single core within the reference area (some 5 kilometres away). Although I am aware that core retrieval is not obvious in deep sea conditions, replication of sediment cores is essential for the conclusion reached (solid phase

Mn can be used as to determine the disturbance/removal depth). This can only be done if the variation within the disturbed area and the reference area is sufficiently small. In order to obtain an uncertainty on the estimated disturbance depth one should compare replicate cores within the disturbed track and reference area.

Author's response: We agree with the referee's objection that more sediment cores from adjacent undisturbed sites and duplicate/triplicate sediment cores from the disturbance tracks would certainly increase the robustness of our study. However, due to the fact there was a large interdisciplinary scientific team participating during cruise SO239, it was not feasible to use more MUC sediment cores for geochemical investigations. Furthermore, retrieving undisturbed/natural sediment cores adjacent to the disturbance track is only possible using ROV-operated push cores with visual control of where the cores are taken (in this case: to be sure to not hit the disturbance track), which can only be performed with a very limited amount of push cores (due to the storage space on the ROV during the dive).

Although, we certainly would like to have more analytical data from replicate sediment cores in order to strengthen the study, geochemical data of pore-water and sediment generally give an integrated signal at least over several tens of meter – especially in deep-sea environments at sites distal to seamounts, so that we are confident that our data is representative for the area and the impact of the disturbances.

[4] The text speaks throughout refers to “mining-related removal” of sediments, while in these seabed trials it is in fact the “mining-related displacement” of sediment, as trenches are made and sediment is simply pushed aside (with a limited resuspension that carries sediment far away, it appears). The bio geochemical consequences of the deposition are not studied (and not discussed). Somehow the aspect of removal is considered more important than the side way deposition part. Moreover, how relevant is this “removal operation” for the envisioned mining approaches? I guess that for actual mining operations, filtering and sorting of polymetallic nodules will happen right at the seafloor (5-20 cm of sediment removal would imply huge volumes to be transported), and so the deposition part will also equally crucial (sediment will be deposited behind the nodule collection vessel?)

Author's response: As described in Chapter 3.1, based on the visual impact inspection, the sediment surface was scraped off during the small-scale disturbance experiments and then indeed pushed aside/piled up next to the freshly exposed sediment surface. We only have taken/studied sediment cores from the freshly exposed sediment surface and not from the pushed-aside sediment pile for several reasons: (1) biological sampling also focused on the freshly exposed sediment surface, and thus, we ensure that we can compare/match biological and geochemical data sets. (2) “mining-related sediment removal” may be the more likely/important scenario for the impact of large-scale industrial deep-sea mining activities than “mining-related sediment displacement” (in the sense of pushed aside/piled up sediments), because current mining technology aims at sucking up nodules and sediment. As mining-related activities will disturb a much larger seafloor area on the scale of km², “mining-related sediment displacement” in the sense of pushed aside/piled up sediments will most probably not play a significant role as the mining equipment will probably disturb these pushed-aside/piled-up sediments again. However, as mentioned in lines 80-83, there is no clear consensus on the most appropriate mining techniques for the industrial exploitation of manganese nodules so far, and thus, the prediction of the environmental consequences including the displacement/removal/resuspension of sediments is difficult. To our knowledge, current literature on mining-related environmental impacts cited in the presented manuscript does not consider “mining-related sediment displacement” in the sense of pushed aside/piled up sediments as a major impact.

We certainly agree that the transport of re-suspended sediment after the disturbance and during industrial filtering/sorting as well as bottom blanketing during/after the disturbance is key for the evaluation of mining-related environmental consequences and especially for biogeochemical conditions and processes in the sediments. However, during the studied small-scale disturbance experiments probably much less sediment was re-suspended than what is to be expected during large-scale industrial deep-sea mining activities. The studied old benthic impact experiments do not allow studying of this important environmental aspect. We are currently working on this topic as part of the new JPI Oceans project “Environmental Impacts and Risks of Deep-Sea Mining” (MiningImpactII), which aims at independently accompanying an industrial mining trial.

[5] The description of what model simulations are performed and how these simulations are carried out is lacking in the methods section (or alternatively at the start of section 3.4). So the reader does not know what is actually simulated in Figs 5 and 6. In essence, one first fits steady state depth profiles to the data depth profiles of the undisturbed site (how is this done? E.g. what is the goodness of fit criterion?). Secondly, one removes the top L centimeter in the model domain, keeping the boundary conditions constant. Subsequently, one performs a transient simulation until a new steady state is reached. This simulation procedure should be clearly described.

Author's response: We have added the description of the model simulations in section 2.4. as follows:

“We have applied a transient transport-reaction model for the sites in the BGR-RA and IOM areas (Table 1). These sites were chosen due to distinctively different sedimentation rates and OPD (Table 2). We have adapted the code of the steady state transport-reaction model, which was originally presented by Volz et al. (2018) and used pore-water oxygen, NO₃⁻, Mn²⁺ and NH⁴⁺ data as well as TOC contents of GC sediment cores from the same study as undisturbed reference data (Table 1; Table 2). Thus, the model parameters and baseline input data used for the transient transport-reaction model are the same as presented in the study by Volz et al. (2018).”

Furthermore, we have added a sentence in the figure caption of figure 5 that the analytical data shown in the graph represents the undisturbed/baseline data as following:

“Figure 5: Model results of the transient transport-reaction model for (a) the EBS disturbance in the German BGR-RA area and (b) the IOM-BIE disturbance in the eastern European IOM area. The model is adapted after the steady state transport-reaction model presented in Volz et al. (2018) and shows the response of the geochemical system in the sediments if steady state conditions are disturbed by the removal of the upper 10 cm (BGR-RA, average disturbance depth of BGR-PA and BGR-RA; cf. Table 3) and 7 cm (IOM; Table 3) of the sediments while maintaining the same boundary conditions but with reduced bioturbation over the first 100 years after the disturbance.”

[6] Lines 214. Wrong definition of porosity. The porosity is always defined as the volume of the pore water (including dissolved salts) over the total volume, and hence not the salt-free volume fraction. Moreover, the porosity cannot be determined gravimetrically in a direct fashion. One determines the H₂O content of the sediment gravimetrically as well as the solid phase density. From this and salinity one can calculate porosity (accounting for salt content of pore water).

Author's response: We have adapted this part as follows:

“The mass percentage of the pore water was determined gravimetrically before and after freeze drying of the wet sediment samples.”

Model comments:

Figure 6 is a zoomed-in version of figure 5. Why is the data not plotted on figure 6 (as in figure 5)? Even if the data is off, it is highly instructive to include the data in the plot.

Author's response: We have added the analytical data in figure 6.

Sup Fig 1. Why is the porosity data fitted in such a poor way? Panel a: Why use an exponential if the data is constant? Panel b: the value at infinity should be 0.71 and not 0.65.

Author's response: As pointed out in lines 281-287, the porosity is commonly following an exponential decrease in transport-reaction models indicative of the compacting sediment. However, we agree with the referee's objection that the porosity fit could be improved. We decided against changing the already published porosity parameterization presented in Volz et al., 2018, DSR I for two reasons: (i) The transient model results simulating the removal of the surface layer presented here should be directly comparable to the previously published steady state model results for undisturbed/natural sediments and (2) while the porosity fit towards deeper sediments appears to be 'off' by about 0.03 porosity units, the difference would not alter the overall outcome of the model.

Figure 6. In both panels a and b, the final steady state does not return to the initial state (difference between red and dark blue curves). Explain better what the initial state is, and why this happens.

Author's response: As indicated in the legend of figure 6, the red profile represents the simulation results for 1 day after the surface sediment layer has been removed (see Table 3 for disturbance depth). Thus, the red profile does not indicate the initial steady state geochemical conditions in undisturbed sediments. In order to clarify this, we have added another profile for the simulation of pre-disturbance steady state geochemical conditions and alter the legend accordingly.

In Fig 6 panel b (IOM-Bie site), the organic matter decreases almost linearly with depth. This is rather strange behavior (should be an exponential decrease)

Author's response: As explained in lines 288-290, organic matter was treated as three reactive fractions (3G) in the transport-reaction model including labile, degradable and refractory fractions. The exponential decrease of simulated organic matter contents in the top sediments (due to the presence of different reactive fractions) and below is common during diagenetic modelling (see Arndt et al., 2013, ESR, <http://dx.doi.org/10.1016/j.earscirev.2013.02.008>; Mewes et al., 2016, EPSL, <http://dx.doi.org/10.1016/j.epsl.2015.10.028>; Volz et al., 2018, DSR I;). As only refractory organic matter is left at depth, the curvature might be difficult to see.

Why are there no pore water NH4 data collected? This would provide a strong model constraint on the N cycle (which is now unconstrained, as only a depth profile of NO3 is available)

Author's response: We agree with the referee's objection and we have tried to measure pore-water ammonia onboard (flow-injection method) using fresh untreated pore-water splits as well as in the home lab using frozen samples (-20°C) with the ortho phtalaldehyde (OPA) method in a QuAAtro continuous segmented flow analyzer (Seal Analytical) for low concentration ranges of 0–5 µM. Unfortunately, the concentrations of pore-water ammonia were mostly below detection limit. We assume that ammonia is immediately oxidized to nitrite/nitrate under oxic conditions and therefore it cannot be detected using these methods.

Terminology:

Why are the disturbances referred to as "small-scale disturbance"? The areal coverage of the disturbance is not relevant for the disturbance depth and recovery time, only the vertical impact matters. The disturbance to the sediment geochemistry (and recovery time) is equally large when doing a single track than when doing a whole area covered by multiple tracks. The use of

“small-scale” throughout the ms seems to suggest that large-scale application would have different impacts and recovery times (which should not be the case).

Author’s response: We do not agree with the referee’s objection. It is important to point out that the presented study focuses on the impact of small-scale disturbances because it can only be considered an approximation to the environmental impact of industrial-scale mining activities. Coming back to major comment [4] by referee #2, the presented small-scale disturbances scraped off the sediments, which were then pushed aside and piled up next to the freshly exposed sediment surface. As described before, this “mining-related sediment displacement” will most probably not be the case during industrial-scale mining activities. As mentioned before, presumably much less sediments were re-suspended during the small-scale disturbances presented in this study than what is to be expected by industrial-scale mining activities. While the effect of bottom blanketing by re-suspended sediments on biogeochemical processes within the small-scale disturbance tracks can be mostly neglected, it certainly has to be considered when investigating industrial-scale mining activities. In addition, in the presented study, we show that porosity is not affected by significant sediment compaction from the weight of the disturbance device. Industrial mining equipment is expected to be much heavier than the disturbance devices used during the small-scale disturbance experiments presented in this study. Also lateral effects (e.g. transport of solutes, easier recolonization by fauna and resulting bioturbation) play some role for the single (2-m wide) tracks compared to large-scale industrial disturbances with widths of hundreds of meters to kilometers.

For these reasons, we would prefer to keep the distinction of “small-scale disturbance” throughout the presented manuscript.

The state of the sediment is referred to as “equilibrium”, and this is not a proper word choice. Equilibrium refers to a closed system that does not change. Steady state is the proper term for an open system that does not change. Sediments are open systems.

Author’s response: We have replaced “re-equilibration/equilibrium” by “the system will return to (new) steady state geochemical conditions” accordingly.

Other comments:

The title is not so descriptive for the results presented. May well be changed to “Disturbance depth and recovery time of sediment geochemistry in Clarion-Clipperton zone after surface disturbance”

Author’s response: We do not agree with the referee’s objection. Indeed, we are determining the disturbance depth as it represents a crucial input parameter for the application of the transport-reaction model. However, as described in lines 406-412, the determined disturbance depths as part of this study are well within the range of previous estimates for the disturbance depths, and therefore, it is not a new finding. Using the transport-reaction model, we present estimates for how long it takes until the sedimentary geochemical system reaches steady state conditions. As pointed out in lines 125-127, our second main goal is to assess the consequences of the disturbance on redox zonation and element fluxes, which are presented in Figures 7 and 8.

For these reasons, we would prefer to keep the title.

L1 Title: “element fluxes” -> no element fluxes are determined

Author’s response: Fluxes of oxygen, nitrate and ammonia are presented in Figure 7.

L26 conceived -> understood

Author’s response: We have changed this accordingly.

L49 sediments -> sediment

Author’s response: We have changed this accordingly.

L51 millennium-scale

Author's response: We have change this accordingly.

L51 It does not matter whether these experiments are small-scale -> the areal extent does not influence the recovery time

Author's response: We do not agree with the referee's objection. It is important to point out that the presented study focuses on the impact of small-scale disturbances because it can only be considered an approximation to the environmental impact of industrial-scale mining activities for reasons pointed out in the first comment of referee #2 in Terminology.

L81 delete ref to ms under review

Author's response: We have changed this reference to Hauquier et al., 2019.

L96 estimates

Author's response: We have changed this accordingly.

L132 - The sampling description is unclear – both the disturbed and undisturbed sites were visited on the same cruise. The way the text is written confounding and suggests otherwise.

Author's response: We do not fully understand the referee's objection. In lines 131-135, we clearly state that MUC and GC cores are taken from undisturbed reference sites while video-guided PC cores were taken within the disturbance tracks. In addition to the sampling description, we present all studied sediment cores with the information of type and age of the disturbance for the PC cores in Table 1.

Therefore, we feel like the sampling description is clearly presented.

L158 ...with Mn nodules varying in size and spatial density...

Author's response: We have changed this accordingly.

L189 repetitious

Author's response: We have deleted this sentence.

L194 the mass of an object (expressed in kg) is independent of depth or pressure

Author's response: We have deleted "under normal atmospheric pressure" accordingly.

L238 What is negligible? Less than ?? %

Author's response: The line number seems to be incorrect - we are not sure what is meant here.

L247 subscript i is missing for x and y symbols in formula

Author's response: We have inserted subscript i for x and y accordingly.

L261 delete double ref

Author's response: We have deleted the double reference.

L266 We have adapted the model...-> adapted in what way?

Author's response: The code was adapted from steady state to transient, while the model parameters are same as presented in Volz et al., 2018, DSR I. We have added this in the model description in section 2.4 as follows: "We have adapted the code of the steady state transport-reaction model, which was originally presented by Volz et al. (2018) and used pore-water oxygen, NO₃⁻, Mn²⁺ and NH⁴⁺ data as well as TOC contents of GC sediment cores from the same study as undisturbed reference data (Table 1; Table 2). Thus, the model parameters and baseline input data used for the transient transport-reaction model are the same as presented in the study by Volz et al. (2018)."

L268 It is unclear how the steady model was fitted to the data. See comment above.

Author's response: We have added to the model description in section 2.4 as follows:

"We have adapted the code of the steady state transport-reaction model, which was originally presented by Volz et al. (2018) and used pore-water oxygen, NO₃-, Mn²⁺ and NH₄⁺ data as well as TOC contents of GC sediment cores from the same study as undisturbed reference data (Table 1; Table 2). Thus, the model parameters and baseline input data used for the transient transport-reaction model are the same as presented in the study by Volz et al. (2018)."

Simulated profiles were fitted to the data by adjusting the fitted parameters listed in the Supplementary Table 2.

Eq (5) : the assumption in the model is steady state compaction (porosity not dependent on time) – should be mentioned

Author's response: It is mentioned in lines 281-283.

L293 Eq(8) + is missing in formula

Author's response: There is no Eq. 8 throughout the manuscript so we are not sure what is meant here.

L333 Total bulk Mn contents in the upper 25 cm -> strange term. I guess one implies "Mean solid-phase Mn content in the upper 25 cm"

Author's response: We have adjusted this sentence as follows:

"Bulk Mn contents in the upper 25 cm of the sediments at the disturbed sites are between 0.1 and 0.9 wt% (Fig. 3)."

We are giving the range of Mn contents in the sediments, not the mean value.

Fig 1. Mention in caption what the white areas denote. Add black lines around green areas for clarity.

Author's response: We have changed this accordingly.

Table 2 POC flux -> mg C m⁻² d⁻¹

Author's response: We have changed this accordingly.

Table 3. r_Mn : is this the maximal value? How is this value determined – see comment above

Author's response: In lines 245-248, we explain that "the highest positive linear correlations of solid-phase Mn contents ($r_{Mn} \sim 1$) between the disturbed sites and the respective undisturbed reference sites (Table 1) were used to determine the depths of the disturbances." Thus, the maximum r value is used. We have added this in the table caption as follows:

"Table 3: Calculated Pearson correlation coefficients r_{Mn} and r_{TOC} for the determination of the disturbance depth of various small-scale disturbances investigated in the framework of this study (compare Table 1). For both correlations, the highest positive linear Pearson coefficient for solid-phase Mn contents ($r_{Mn} \sim 1$) between the disturbed sites and the respective undisturbed reference sites was used."

L392 "regional phenomenon" -> what is meant by this: that it is only local or that it common across a broad area of the CCZ? How big is the region?

Author's response: We have changed this sentence accordingly to:

"The fact that the solid-phase Mn maxima in the surface sediments appear to be a regional phenomenon across the CCZ area as it has been observed throughout the different exploration areas studied in the framework of this study (Volz et al., in press)"

L413 "were removed" -> but also placed just on the side of the track

Author's response: We have added “...and pushed aside”.

L468 “Ming-related removal” Is this really mining-related? Is it removal? As it placed just on the side of the track...

Author's response: We have deleted “mining-related”. As we are studying only sediment cores from the (freshly) exposed sediment surface after the sediment has been scraped off (lines 312-314), we feel confident that we can talk about sediment removal.

L473. Which organisms are the dominant bioturbators? This is crucial information to provide insight into their return time? Large motile surface-dwellers (e.g. sea cucumbers) may return faster...

Author's response: We agree with the referee's objection that it would be important to know which organisms are the dominant bioturbators in sediments of the CCZ. To our knowledge, data/studies on this topic are very rare for the deep sea and do not exist for the CCZ. Therefore, we have pointed out in lines 293-302, “due to the lack of data on the re-establishment of bioturbation, i.e. the recovery of the bioturbation ‘pump’ after small-scale disturbance experiments, we have tested the effect of different bioturbation scenarios in the transport-reaction model. For the different post-disturbance bioturbation scenarios, we have assumed that bioturbation is inhibited immediately after the disturbance with a linear increase to undisturbed reference bioturbation coefficients (Volz et al., 2018). Based on the work by Miljutin et al. (2011) and Vanreusel et al. (2016), we have assumed that bioturbation should be fully re-established after 100, 200, and 500 yr. As the modelling results for the different time spans were almost identical, we only present here the model that assumes bioturbation is at pre-disturbance intensity 100 yr after the impact (Volz et al., 2018; Supplementary Table 2).”

Thus, this is the best approximation of the re-establishment of bioturbation for the application of a transport-reaction model.

Moreover, is there a point for the bioturbators to return, if the food stock (organic matter) has not yet been replenished? Figure 5 shows that it takes over 10.000 years to get the organic matter back up in the surface layer.

Author's response: As elaborated in the previous response, due to the lack of data on the re-establishment of bioturbation after disturbances, we have tested different post-disturbance bioturbation scenarios in the transport-reaction model based on the work by Miljutin et al. (2011) and Vanreusel et al. (2016). Thus, the time span after which bioturbation is re-established is based on actual biological studies on disturbances in the study area.

Although we are not experts in biology/bioturbators, we think that bioturbators not only return once the surface layer is fully re-established but that they can already return once the surface layer is only partly re-established. At this point, some “fresh” organic matter has been deposited, which is probably a point for bioturbators to return. Vonnahme et al., revised, Science Advances show that microbe abundances may recover on decadal scale, i.e. before the reactive surface layer has been redeposited. Hence, fauna is likely going to graze on those microbes and thus recolonize on decadal time scales as well.

L487 Unclear why denitrification would increase when OPD gets deeper -> explain better

Author's response: We are not saying that denitrification increases once the OPD shifts deeper into the sediment, we are actually implying the opposite: denitrification is weakened in the oxic environment due to the fact that aerobic respiration is favored over denitrification. Therefore we are writing in lines 486-490 that “interestingly, during the transition time (at which point solute profiles slowly shift towards their pre-disturbance shape) when oxygen is still present at depth but aerobic respiration in the upper sediments

has already began to pick up, NO_3^- concentrations are strongly elevated in the BGR sediments (Figs. 5 and 6). This is due to the fact that NO_3^- is not consumed during denitrification or the Mn-annamox reaction in the presence of oxygen (Mogollón et al., 2016; Volz et al., 2018)."

We do not feel that this needs clarification.

L554 (and elsewhere) equilibrium -> steady state (see comment above)

Author's response: We have replaced "re-equilibration/equilibrium" by "the system will return to (new) steady state geochemical conditions" accordingly.

Fig 7. Plot all times on the x-axis

Author's response: The timescale has been added to the figure.

1 **Impact of small-scale disturbances on geochemical conditions, biogeochemical processes**
2 **and element fluxes in surface sediments of the eastern Clarion-Clipperton Zone, Pacific**
3 **Ocean**

4 Jessica B. Volz^{a,*}, Laura Haffert^b, Matthias Haeckel^b, Andrea Koschinsky^c, Sabine Kasten^{a,d}

5 ^a Alfred Wegener Institute Helmholtz Centre for Polar and Marine Research, 27570
6 Bremerhaven, Germany

7 ^b GEOMAR Helmholtz Centre for Ocean Research Kiel, 24148 Kiel, Germany

8 ^c Jacobs University Bremen, Department of Physics and Earth Sciences, 28759 Bremen,
9 Germany

10 ^d University of Bremen, Faculty of Geosciences, Klagenfurter Strasse, 28359 Bremen, Germany

11

12 *Corresponding author:

13 Tel: +49 471 4831 1842

14 Email: Jessica.volz@awi.de

15

16

17

18 **Keywords:** Deep-sea mining, CCZ, polymetallic nodules, redox zonation, oxygen penetration
19 depth, solid-phase manganese

20

21 **Abstract**

22 The thriving interest in harvesting deep-sea mineral resources, such as polymetallic nodules,
23 calls for environmental impact studies, and ultimately, for regulations for environmental
24 protection. Industrial-scale deep-sea mining of polymetallic nodules most likely has severe
25 consequences for the natural environment. However, the effects of mining activities on deep-
26 sea ecosystems, sediment geochemistry and element fluxes are still poorly
27 ~~conceivedunderstood~~. Predicting the environmental impact is challenging due to the scarcity of
28 environmental baseline studies as well as the lack of mining trials with industrial mining
29 equipment in the deep sea. Thus, currently we have to rely on small-scale disturbances
30 simulating deep-sea mining activities as a first-order approximation to study the expected
31 impacts on the abyssal environment.

32 Here, we investigate surface sediments in disturbance tracks of seven small-scale benthic
33 impact experiments, which have been performed in four European contract areas for the
34 exploration of polymetallic nodules in the Clarion-Clipperton Zone (CCZ). These small-scale
35 disturbance experiments were performed 1 day to 37 years prior to our sampling program in the
36 German, Polish, Belgian and French contract areas using different disturbance devices. We
37 show that the depth distribution of solid-phase Mn in the upper 20 cm of the sediments in the
38 CCZ provides a reliable tool for the determination of the disturbance depth, which has been
39 proposed in a previous study (Paul et al., 2018). We found that the upper 5–15 cm of the
40 sediments were removed during various small-scale disturbance experiments in the different
41 exploration contract areas. Transient transport-reaction modelling for the Polish and German
42 contract areas reveals that the removal of the surface sediments is associated with the loss of
43 reactive labile organic carbon. As a result, oxygen consumption rates decrease significantly
44 after the removal of the surface sediments, and consequently, oxygen penetrates up to tenfold
45 deeper into the sediments inhibiting denitrification and Mn(IV) reduction. Our model results
46 show that the ~~post-disturbance return to steady state~~ geochemical ~~re-equilibration conditions~~
47 ~~after the disturbance~~ is controlled by diffusion until the reactive labile TOC fraction in the
48 surface sediments is partly re-established and the biogeochemical processes commence. While
49 the re-establishment of bioturbation is essential, ~~the steady state~~ geochemical ~~re-equilibration~~
50 ~~of the sediments is conditions are~~ ultimately controlled by the burial rates of organic matter.
51 Hence, under current depositional conditions, ~~the new geochemical equilibrium steady state~~
52 ~~geochemical conditions~~ in the sediments of the CCZ is reached only on a millennium-a-scale
53 even for these small-scale disturbances simulating deep-sea mining activities.

54 **1. Introduction**

55 The accelerating global demand for metals and rare-earth elements are driving the economic
56 interest in deep-sea mining (e.g., Glasby, 2000; Hoagland et al., 2010; Wedding et al., 2015).

57 Seafloor minerals of interest include (1) polymetallic nodules (e.g., Mero, 1965), (2) massive
58 sulfide deposits (e.g., Scott, 1987) and (3) cobalt-rich crusts (e.g., Halkyard, 1985). As the
59 seafloor within the Clarion-Clipperton Zone (CCZ) in the NE Pacific holds one of the most
60 extensive deposits of polymetallic nodules with considerable base metal quantities, commercial
61 exploitation of seafloor mineral deposits may focus on the CCZ (e.g., Mero, 1965; Halbach et
62 al., 1988; Rühlemann et al., 2011; Hein et al., 2013; Kuhn et al., 2017a). The exploration, and
63 ultimately, industrial exploitation of polymetallic nodules demands for international regulations
64 for the protection of the environment (e.g., Halfar and Fujita, 2002; Glover and Smith, 2003;
65 Davies et al., 2007; van Dover, 2011; Ramirez-Llodra et al., 2011; Boetius and Haeckel, 2018).
66 The International Seabed Authority (ISA) is responsible for regulating the exploration and
67 exploitation of marine mineral resources as well as for protecting and conserving the marine
68 environment beyond the exclusive economic zones of littoral states from harmful effects (ISA,
69 2010). The ISA has granted temporal contracts for the exploration of polymetallic nodules in
70 the CCZ, engaging all contract holders to explore resources, test mining equipment and assess
71 the environmental impacts of deep-sea mining activities (ISA 2010; Lodge et al., 2014;
72 Madureira et al., 2016).

73 Although a considerable number of environmental impact studies have been conducted in
74 different nodule fields, the prediction of environmental consequences of potential future deep-
75 sea mining is still difficult (e.g., Ramirez-Llodra et al., 2011; Jones et al., 2017; Gollner et al.,
76 2017; Cuvelier et al., 2018). In case of the CCZ, the evaluation of the environmental impact of
77 deep-sea mining activities is challenging due to the fact that baseline data on the natural spatial
78 heterogeneity and temporal variability of depositional conditions, benthic communities and the
79 biogeochemical processes in the sediments are scarce (e.g., Mewes et al., 2014; 2016; Vanreusel
80 et al., 2016; Mogollón et al., 2016; Juan et al., 2018; Volz et al., 2018; Menendez et al., 2018;
81 Hauquier et al., under review 2019). In addition, there is no clear consensus on the most
82 appropriate mining techniques for the commercial exploitation of nodules, and technical
83 challenges due to the inaccessibility of nodules at great water depths between 4000–5000 m
84 have limited the deployment of deep-sea mining systems until today (e.g., Chung, 2010; Jones
85 et al., 2017).

86 The physical removal of nodules as hard-substrate habitats has severe consequences for the
87 nodule-associated sessile fauna as well as the mobile fauna (Bluhm, 2001; Smith et al., 2008;
88 Purser et al., 2016; Vanreusel et al., 2016). With slow nodule growth rates of a few
89 millimeters per million years (e.g., Halbach et al., 1988; Kuhn et al., 2017a), the deep-sea fauna
90 may not recover for millions of years (Vanreusel et al., 2016; Jones et al., 2017; Gollner et al.,
91 2017; Stratmann et al., 2018). In addition to the removal of deep-sea fauna as well as seafloor
92 habitats, the exploitation of nodules is associated with (1) the removal, mixing and re-
93 suspension of the upper 4 cm to more than several tens of centimeters of the sediments, (2) the
94 re-deposition of material from the suspended sediment plume, and (3) potentially also the
95 compaction of the surface sediments due to weight of the nodule collector (Thiel, 2001; Oebius
96 et al., 2001; König et al., 2001; Grupe et al., 2001; Radziejewska, 2002; Khripounoff et al.,
97 2006; Cronan et al., 2010; Paul et al., 2018; Gillard et al., 2019). The wide range of ~~estimations~~
98 estimates for the disturbance depth may be associated with (1) various devices used for the
99 deep-sea disturbance experiments (Brockett and Richards, 1994; Oebius et al., 2001; Jones et
100 al., 2017), (2) distinct sediment properties in different nodule fields of the Pacific Ocean (e.g.,
101 Cronan et al., 2010; Hauquier et al., ~~under review~~2019) as well as (3) different approaches for
102 the determination of the disturbance depth (e.g., Oebius et al., 2001; Grupe et al., 2001;
103 Khripounoff et al., 2006). Based on the observation that bulk solid-phase Mn contents decrease
104 over depth in the surface sediments of the DISCOL area, Paul et al. (2018) have suggested that
105 the depth distribution of solid-phase Mn and associated metals (e.g., Mo, Ni, Co, Cu) could be
106 used to trace the sediment removal by disturbances. In addition, other solid-phase properties
107 such as organic carbon contents (TOC), porosity and radioisotopes may be suitable for the
108 determination of the disturbance depth.

109 The most reactive TOC compounds, found in the bioturbated uppermost sediment layer, are the
110 main drivers for early diagenetic processes (e.g., Froelich et al., 1979; Berner, 1981) and are
111 expected to be removed during mining activities (König et al., 2001). Thus, strong
112 biogeochemical implications can be expected in the sediments after deep-sea mining activities.
113 König et al. (2001) have applied numerical modelling to study the consequences of the removal
114 of the upper 10 cm of the sediments in the DISCOL area in the Peru Basin. They showed that
115 the degradation of TOC during aerobic respiration, denitrification and Mn(IV) reduction may
116 be decreased for centuries ~~strongly influencing increasing~~ the oxygen penetration depth (OPD).

117 Here, we investigate the impact of various small-scale disturbances on geochemical conditions,
118 biogeochemical processes and element fluxes in surface sediments of the CCZ. These small-

119 scale disturbance tracks were created up to 37 years ago in four different European contract
120 areas for the exploration of polymetallic nodules, including the German BGR (Bundesanstalt
121 für Geowissenschaften und Rohstoffe) area, the Belgian GSR (Global Sea Mineral Resources
122 NV) area, the French IFREMER (Institut Français de Recherche pour l'Exploitation de la Mer)
123 area and the Polish IOM (InterOceanMetal) area. In order to determine the disturbance depths
124 of the different small-scale disturbances in the different European contract areas, we correlate
125 the depth distributions of solid-phase Mn and total organic carbon (TOC) between disturbed
126 sites and undisturbed reference sites using the Pearson product-moment correlation coefficient.
127 On this basis, we (1) assess the short- and long-term consequences of small-scale disturbances
128 on redox zonation and element fluxes and (2) determine how much time is needed for the re-
129 establishment of a new steady state geochemical equilibrium system in the sediments after the
130 disturbances. Our work includes pore-water and solid-phase analyses as well as the application
131 of a transient one-dimensional transport-reaction model.

132 2. Material and methods

133 As part of the European JPI Oceans pilot action “Ecological Aspects of Deep-Sea Mining
134 (MiningImpact)”, multiple corer (MUC) and gravity corer (GC) sediment cores were taken
135 during RV SONNE cruise SO239 in March/April 2015 from undisturbed sites in various
136 European contract areas for the exploration of polymetallic nodules (Fig. 1; Table 1; Martínez
137 Arbizu and Haeckel, 2015). These undisturbed reference sites were chosen in close proximity
138 (< 5 km) to small-scale disturbance experiments for the simulation of deep-sea mining, which
139 were created up to 37 yr ago and re-visited during cruise SO239 (Table 1; see Sect. 2.1.1.;
140 Martínez Arbizu and Haeckel, 2015). The sampling of sediments in the disturbance tracks of
141 these experiments were conducted by video-guided push-coring (PC) between 1 day and 37 yr
142 after the initial disturbances using the ROV Kiel 6000 (Table 1; Fig. 2; Martínez Arbizu and
143 Haeckel, 2015).

144 The different investigated European contract areas within the CCZ include the BGR, IOM, GSR
145 and IFREMER areas. Comprehensive pore-water and solid-phase analyses on the MUC and
146 GC sediment cores from undisturbed sites have been conducted in previous baseline studies
147 and are presented elsewhere (Volz et al., 2018; Volz et al., in pressunder review). These
148 analyses include the determination of pore-water oxygen, NO_3^- , Mn^{2+} and NH_4^+ concentrations
149 and contents of total organic carbon (TOC) for MUC and GC sediment cores (Volz et al., 2018)
150 as well as solid-phase bulk Mn contents for the MUC sediment cores (Volz et al., in pressunder
151 review). In the framework of this study, we have used these previously published pore-water

152 and solid-phase data as undisturbed reference data for geochemical conditions and sediment
153 composition (Table 1). On this basis, here, we investigate seven small-scale disturbances for
154 the simulation of deep-sea mining (Table 1; see Sect. 2.1.1.; Martínez Arbizu and Haeckel,
155 2015).

156 **2.1. Site Description**

157 The CCZ is defined by two transform faults, the Clarion Fracture Zone in the north and the
158 Clipperton Fracture Zone in the south and covers an area of about 6 million km² (Fig. 1; e.g.,
159 Halbach et al., 1988). The sediments at the investigated sites (Table 1) are dominated by clayey
160 siliceous oozes with various-Mn nodules varying in sizes (1–10 cm) and spatial densityies (0–
161 30 kg m⁻²) at the sediment surface (Berger, 1974; Kuhn et al., 2012; Mewes et al., 2014; Volz
162 et al., 2018). In order to characterize the investigated sediments with respect to redox zonation,
163 sedimentation rates, fluxes of particulate organic carbon (POC) to the seafloor and bioturbation
164 depths, we have summarized these key parameters, which are originally presented elsewhere,
165 in Table 2 (Volz et al., 2018). Steady state transport-reaction models have shown that aerobic
166 respiration is the dominant biogeochemical process at all investigated sites, consuming more
167 than 90 % of the organic matter delivered to the seafloor (Mogollón et al., 2016; Volz et al.,
168 2018). Below the OPD at more than 0.5 m depth, Mn(IV) and nitrate reduction succeeds in the
169 suboxic zone, where oxygen and sulfide are absent (e.g., Mewes et al., 2014; Mogollón et al.,
170 2016; Kuhn et al., 2017b; Volz et al., 2018). At several sites investigated in this study, including
171 the BGR “reference area” (BGR-RA) and IOM sites, decreasing Mn²⁺ concentrations at depth
172 are probably associated with the oxidation of Mn²⁺ by upward diffusing oxygen circulating
173 through the underlying basaltic crust (Volz et al., 2018; Mewes et al., 2016; Kuhn et al., 2017b).

174 **2.1.1. Small-scale disturbances**

175 Since the 1970s, several comprehensive environmental impact studies of deep-sea mining
176 simulations have been carried out in the CCZ, including the Benthic Impact Experiment (BIE;
177 e.g., Trueblood and Ozturgut, 1997; Radziejewska, 2002) and the Japan Deep Sea Impact
178 Experiment (JET; Fukushima, 1995). In addition, numerous small-scale seafloor disturbances
179 have been carried out in the CCZ in the past 40 yr using various tools such as epibenthic sleds
180 (EBS) and dredges (e.g., Vanreusel et al., 2016; Jones et al., 2017). The EBS is towed along the
181 seabed for the collection of benthic organisms (and nodules) thereby also removing the upper
182 few centimeters of the sediments (e.g., Brenke, 2005). In 2015, some of these up to 37 yr old
183 disturbances were re-visited as part of the BMBF-EU JPI Oceans pilot action “Ecological
184 Aspects of Deep-Sea Mining (MiningImpact)” project in order to evaluate the long-term

185 consequences of such small-scale disturbances on the abyssal benthic ecosystem (Table 1;
186 Fig. 2; Martínez Arbizu and Haeckel, 2015). For comparison, the Disturbance and
187 Recolonization Experiment (DISCOL), which was conducted in a nodule field in the Peru Basin
188 (PB) in 1989 was re-visited as part of MiningImpact (Boetius, 2015; Greinert, 2015). In the
189 framework of DISCOL, a seafloor area of ~ 11 km² was disturbed with a plough harrow. The
190 impact of the DISCOL experiment was studied 0.5, 3 and 7 yr after the disturbance had been
191 set (e.g., Thiel, 2001).

192 ~~Comparably small scale, up to 37 yr old simulations of deep-sea mining in various European
193 contract areas within the CCZ were re-visited in 2015 during the RV SONNE cruise SO239
194 (Table 1; Fig. 2; Martínez Arbizu and Haeckel, 2015). Furthermore, N~~ew small-scale
195 disturbance tracks were created during SO239 in the BGR-RA and in the GSR area “B6” using
196 an EBS in order to add also initial temporal datasets (Table 1; Fig. 2; Martínez Arbizu and
197 Haeckel, 2015). The EBS weighed about 400 kg ~~under normal atmospheric pressure~~ and created
198 a disturbance track of about 1.5 m width (Brenke, 2005). The fresh EBS disturbance tracks in
199 the BGR-RA and GSR areas were re-visited 1 day after their creation. Eight months prior to the
200 cruise SO239, towed dredge sampling was performed in the GSR area by the Belgian contractor
201 (Martínez Arbizu and Haeckel, 2015; Jones et al., 2017). During the BIONOD cruises onboard
202 RV L’Atalante in 2012, the same EBS setup as used during cruise SO239 was deployed in the
203 BGR “prospective area” (BGR-PA) and in the IFREMER area (Table 1; Rühlemann and Menot,
204 2012; Menot and Rühlemann, 2013; Martínez Arbizu and Haeckel, 2015). In 1995, the Deep-
205 Sea Sediment Re-suspension System (DSSRS) was used during the IOM-BIE (Benthic Impact
206 Experiment) disturbance in the IOM area (Table 1; e.g., Kotlinski and Stoyanova, 1998). The
207 DSSRS weighed 3.2 tons under normal atmospheric pressure and was designed to dredge the
208 seafloor while producing a re-suspended particle plume about 5 m above the seafloor (Brockett
209 and Richards, 1994; Sharma, 2001). Based on the dimensions of the DSSRS device, the
210 disturbance track created during the IOM-BIE disturbance experiment is about 2.5 m wide
211 (Fig. 2; Brockett and Richards, 1994). In 1978, the Ocean Mineral Company (OMCO) created
212 disturbance tracks in the French IFREMER area by towed dredge sampling (Table 1; e.g.,
213 Spickermann, 2012).

214 2.2. Sediment sampling and solid-phase analyses

215 ROV-operated push cores were sampled at intervals of 1 cm for solid-phase analyses. Bulk
216 sediment data and TOC contents have been corrected after Kuhn (2013) for the interference of
217 the pore-water salt matrix with the sediment composition (Volz et al., 2018). The ~~salt free~~

218 ~~volume fraction mass percentage~~ of the pore water, i.e. the porosity, was determined
 219 gravimetrically before and after freeze drying of the wet sediment samples. The salt-corrected
 220 sediment composition c' was calculated from the measured solid-phase composition c using the
 221 mass percentage of H_2O of the wet sediment (w), which contains 96.5 % H_2O (Eq. (1)).

$$222 \quad c' = c * \frac{100}{100 - (100 * \frac{(w * \frac{100}{96.5}) - w}{100 - w})} \quad (1)$$

223 2.2.1. Total acid digestions

224 Total acid digestions were performed in the microwave system MARS Xpress (CEM) after the
 225 protocols by Kretschmer et al. (2010) and Nöthen and Kasten (2011). Approximately 50 mg of
 226 freeze-dried, homogenized bulk sediment were digested in an acid mixture of 65 % sub-boiling
 227 distilled HNO_3 (3 mL), 30 % sub-boiling distilled HCl (2 mL) and 40 % suprapur®
 228 HF (0.5 mL) at ~ 230 °C. Digested solutions were fumed off to dryness, the residue was re-
 229 dissolved under pressure in 1 M HNO_3 (5 mL) at ~ 200 °C and then filled up to 50 mL with
 230 1 M HNO_3 . Total bulk Mn and Al contents were determined using inductively coupled plasma
 231 optical emission spectrometry (ICP-OES; IRIS Intrepid ICP-OES Spectrometer, Thermo
 232 Elemental). Based on the standard reference material NIST 2702 accuracy and precision of the
 233 analysis was 3.7 % and 3.5 % for Mn, respectively ($n=67$).

234 2.2.2. Total organic carbon

235 Total organic carbon (TOC) contents were determined using an Eltra CS2000 element analyzer.
 236 Approximately 100 mg of freeze-dried, homogenized sediment were transferred into a ceramic
 237 cup and decalcified with 0.5 mL of 10 % HCl at 250 °C for 2 h before analysis. Based on an in-
 238 house reference material, precision of the analysis was better than 3.7 % ($n=83$).

239 2.3. Pearson correlation coefficient

240 In order to determine the disturbance depths, solid-phase bulk Mn contents were correlated
 241 between disturbed sediments and undisturbed reference sediments using the Pearson product-
 242 moment correlation coefficient r (Eq. (2); Table 1; Pearson, 1895). The Pearson correlation
 243 coefficient is a statistical measure of the linear relationship between two arrays of variables
 244 with:

$$245 \quad r_{xy} = \frac{\sum_{i=1}^n (x_i - \bar{x})(y_i - \bar{y})}{\sqrt{\sum_{i=1}^n (x_i - \bar{x})^2 \sum_{i=1}^n (y_i - \bar{y})^2}} \quad (2)$$

247 where n is the sample size, x and y are individual sample points and \bar{x} and \bar{y} are the sample
 248 means $\bar{x} = \frac{1}{n} \sum_{i=1}^n x_i$ and $\bar{y} = \frac{1}{n} \sum_{i=1}^n y_i$.

249 While the solid-phase bulk Mn contents of the disturbed sediments were determined in the
 250 framework of this study, solid-phase bulk Mn contents from undisturbed reference sediments
 251 were taken from Volz et al. (in press under review). The highest positive linear correlations of
 252 solid-phase Mn contents ($r_{\text{Mn}} \sim 1$) between the disturbed sites and the respective undisturbed
 253 reference sites (Table 1) were used to determine the depths of the disturbances. In a second
 254 step, the same correlation was applied to the TOC contents (r_{TOC}) in order to verify the depth
 255 of disturbance. While the TOC contents in the disturbed sediments were determined in the
 256 framework of this study, TOC contents from undisturbed reference sediments were taken from
 257 Volz et al. (2018).

258 **2.4. Geochemical model setup and reaction network**

259 A transient one-dimensional transport-reaction model (Eq. (3); e.g., Boudreau, 1997; Haeckel
 260 et al., 2001; Boudreau, 1997) was used (1) to assess the impact of small-scale disturbances on
 261 biogeochemical processes, geochemical conditions and element fluxes in sediments of the CCZ
 262 and (2) to estimate the time required to establish a new steady state geochemical equilibrium
 263 system after a small-scale disturbance. We have applied the a transient transport-reaction
 264 model for the sites in the BGR-RA and IOM areas (Table 1). These sites were chosen due to
 265 distinctively different sedimentation rates and OPD (Table 2). We have adapted the code of the
 266 steady state transport-reaction model, which was originally presented by Volz et al. (2018) and
 267 used pore-water oxygen, NO_3^- , Mn^{2+} and NH_4^+ data as well as TOC contents of GC sediment
 268 cores from the same study as undisturbed reference data (Table 1; Table 2). Thus, the model
 269 parameters and baseline input data used for the transient transport-reaction model are the same
 270 as presented in the study by Volz et al. (2018). The transient transport-reaction model consists
 271 of four aqueous (O_2 , NO_3^- , Mn^{2+} , NH_4^+), four solid species (TOC_{1-3} , MnO_2) and six reactions
 272 (R₁-R₆; Supplementary Table 1) with:

$$273 \frac{\partial(\vartheta_i C_{i,j})}{\partial t} = \frac{\partial D_{i,j} \vartheta_i (\partial C_{i,j} / \partial z)}{\partial z} - \frac{\partial \omega_i \vartheta_i C_{i,j}}{\partial z} + \alpha_i \vartheta_i (C_{i,j} - C_{0,j}) + \vartheta_i \sum R_{i,j} \quad (3)$$

274 where z is sediment depth, and subscripts i, j represent depth and species-dependence,
 275 respectively; aqueous or solid species concentration are denoted by C (Supplementary Table
 276 2); D is in case of solutes the effective diffusive mixing coefficient, which has been corrected
 277 for tortuosity ($D_{m,i,j}$; Boudreau, 1997). In the case of solids, D represents the bioturbation

278 coefficient (B_i ; Eq. (4)); ϑ is the volume fraction representing the porosity φ for the aqueous
279 phase and $1 - \varphi$ for the solid phase; the velocity of either the aqueous (v) or the solid phase
280 (w) is denoted by the symbol ω ; α_i is the bioirrigation coefficient (0 for solid species; Eq. (5));
281 and $\sum R_{i,j}$ is the sum of the reactions affecting the given species.

282 The bioturbation and bioirrigation profiles, i.e. biologically induced mixing of sediment and
283 pore water, respectively, are represented by a modified logistic function:

$$284 B_i = B_0 \exp\left(\frac{z_{mix} - z_i}{z_{att}}\right) / \left(1 + \exp\left(\frac{z_{mix} - z_i}{z_{att}}\right)\right) \quad (4)$$

$$285 \alpha_i = \alpha_0 \exp\left(\frac{z_{mix} - z_i}{z_{att}}\right) / \left(1 + \exp\left(\frac{z_{mix} - z_i}{z_{att}}\right)\right) \quad (5)$$

286 where α_0 and B_0 are constants indicating the maximum bioirrigation and bioturbation intensity
287 at the sediment-water interface; the depth where the bioturbation and bioirrigation intensity is
288 halved is denoted by z_{mix} ; and the attenuation of the biogenically induced mixing with depth
289 is controlled by z_{att} .

290 Assuming steady-state compaction, the model applies an exponential function that is
291 parameterized according to the available porosity data at each station (e.g., Berner, 1980;
292 Supplementary Fig. 1):

$$293 \varphi_i = \varphi_\infty (\varphi_0 - \varphi_\infty) \exp(-\beta z) \quad (6)$$

294 where φ_∞ is the porosity at the ‘infinite depth’, at which point compaction is completed; φ_0 is
295 the porosity at the sediment water interface ($z = 0$); and β is the porosity-attenuation
296 coefficient.

297 Organic matter was treated in three reactive fractions (3G-model) with first order kinetics. The
298 rate expressions for the reactions (R_1 - R_6) include inhibition terms, which are listed together
299 with the rate constants (Supplementary Table 3).

300 Based on the Pearson correlation coefficient r_{Mn} , we have removed the upper 7 cm of sediments
301 in the transport-reaction model for the IOM-BIE site and the upper 10 cm of sediments in the
302 transport-reaction model for the BGR-RA site. Due to the lack of data on the re-establishment
303 of bioturbation, i.e. the recovery of the bioturbation ‘pump’ after small-scale disturbance
304 experiments, we have tested the effect of different bioturbation scenarios in the transport-
305 reaction model. For the different post-disturbance bioturbation scenarios, we have assumed that
306 bioturbation is inhibited immediately after the disturbance with a linear increase to undisturbed
307 reference bioturbation coefficients (Volz et al., 2018). Based on the work by Miljutin et al.

308 (2011) and Vanreusel et al. (2016), we have assumed that bioturbation should be fully re-
309 established after 100, 200, and 500 yr. As the modelling results for the different time spans
310 were almost identical, we only present here the model that assumes bioturbation is at pre-
311 disturbance intensity 100 yr after the impact (Volz et al., 2018; Supplementary Table 2). We
312 have applied the transient transport-reaction model under the assumption that the sedimentation
313 rates as well as the POC fluxes to the seafloor remain constant over time (Table 2). The model
314 was coded in MATLAB with a discretization and reaction set-up closely following the steady
315 state model (Volz et al., 2018).

316 **3. Results**

317 **3.1. Characterization of disturbed sites**

318 Most of the small-scale disturbances investigated in the framework of this study were created
319 with an EBS (Table 1; Fig. 2). Based on the visual impact inspection of the EBS disturbance
320 tracks in the CCZ, the sediments were mostly pushed aside by the EBS and piled up next to the
321 left and right of the tracks (Fig. 2). In particular, the freshly created 1-day old EBS tracks in the
322 BGR-RA and GSR areas indicate that the sediments were mostly scraped off and accumulated
323 next to the freshly exposed sediment surfaces (Fig. 2). Small sediment lumps occur on top of
324 the exposed sediment surfaces on the EBS tracks, which indicates that some sediment has slid
325 off from the adjacent flanks of the sediment accumulation after the disturbances (Fig. 2).
326 However, the mostly smooth sediment surfaces of the EBS tracks suggest that sediment mixing
327 during the EBS disturbance experiments may be mostly negligible (Fig. 2; Table 1). In the 8-
328 months old dredge track in the GSR area, small furrows occur at the disturbed sediment surface
329 most likely caused by the shape of the dredge (Fig. 2).

330 **3.2. Sediment porosity and solid-phase composition**

331 The sediment porosity shows little lateral variability and ranges between 0.65 and 0.8
332 throughout the upper 25 cm of the sediments at all investigated disturbed sites (Fig. 3). At the
333 disturbed IOM-BIE site, sediment porosity is about 5 % higher in the upper 4 cm of the
334 sediments than below. ~~Total-b~~_{Bulk} Mn contents in the upper 25 cm of the sediments at the
335 disturbed sites are between 0.1 and 0.9 wt% (Fig. 3). Solid-phase Mn contents decrease with
336 depth at all investigated sites. Total organic carbon (TOC) contents in the upper 25 cm of the
337 sediments at the disturbed sites are within 0.2 and 0.5 wt% (Fig. 3). The TOC contents slightly
338 decrease with depth at all investigated sites.

339 **3.3. Pearson correlation coefficient and disturbance depths**

340 The Pearson correlation coefficient r_{Mn} for the correlation of solid-phase Mn contents between
341 the disturbed sites and the respective reference sites ranges between 0.72 and 0.97 (Table 3).
342 Based on r_{Mn} , 5-15 cm of sediment has been removed by various disturbance experiments in
343 the different contract areas (Fig. 4). Applying these r_{Mn} -derived disturbance depths for the
344 correlation of the TOC depth distributions between disturbed sites and respective adjacent
345 reference sites gives Pearson correlation coefficients r_{TOC} within 0.73 and 0.91 (Table 3;
346 Fig. 4), which may support the estimates for the disturbance depth based on r_{Mn} . At the BGR-
347 RA site, the correlation of TOC contents between the disturbed site and the reference site shows
348 negative values. As the sediment porosity in the disturbed sediments correlates well with the
349 porosity in the respective undisturbed reference sediments (Fig. 4), sediment compaction due
350 to the weight of the disturbance device may be negligible during the small-scale disturbances
351 investigated in the framework of this study.

352 **3.4. Transport-reaction modelling**

353 The removal of the surface sediments in the transient transport-reaction model for the BGR-RA
354 and IOM-BIE sites is associated with the loss of the reactive labile organic matter (Fig. 5 and 6).
355 About 10 kyr after the removal of the upper 10 cm of the sediments in the model for the BGR-
356 RA site, oxygen penetrates about tenfold deeper into the disturbed sediments than in
357 undisturbed sediments (Table 2; Fig. 5; Volz et al., 2018). At the IOM-BIE site, oxygen reaches
358 the maximum OPD at about 100 yr after the removal of the upper 7 cm of the sediments. At
359 this site, the oxygen front migrates only ~ 1 m deeper than the corresponding OPD in
360 undisturbed sediments (Table 2; Fig. 5; Volz et al., 2018). As a consequence of deeper OPDs
361 at both sites, the oxic-suboxic redox boundary is located at greater depth, with a significant
362 consumption of pore-water Mn^{2+} in the path of the oxygen front. The NH_4^+ concentrations are
363 also being diminished, reaching minima within 100-1000 yr and 1-10 yr after the disturbance
364 experiments in the BGR-RA and IOM areas, respectively. The trend for the NO_3^- is more
365 complicated with lower concentrations during the downward migration of the OPD and
366 augmented concentrations once oxygen concentrations reach their maximum (Figs. 5 and 6).

367 Naturally, the solute fluxes across the sediment-water interface (SWI) are strongly affected after
368 the surface sediment removal (Fig. 7). The transient transport-reaction model suggests that the
369 oxygen fluxes into the sediments are lowered by a factor of three to six after 10-100 yr at the
370 IOM-BIE and BGR-RA sites, respectively. This trend is mirrored by the decreased release of
371 NH_4^+ and NO_3^- into the bottom water.

372 **4. Discussion**

373 **4.1. Depths of small-scale disturbance experiments**

374 Our work demonstrates that the depth distribution of solid-phase Mn provides a reliable tool
375 for the determination of the disturbance depths in the sediments of the CCZ (Fig. 4; Table 3).
376 The success of the correlation of solid-phase Mn contents between disturbed and undisturbed
377 reference sediments benefits from several factors:

378 (1) Sediment mixing during the small-scale disturbance experiments is negligible: The visual
379 impact assessment of the investigated disturbance tracks in the CCZ suggests that sediment
380 mixing during the small-scale disturbance experiments was insignificant (Fig. 2). This
381 observation is in agreement with a recent EBS disturbance experiment, which has been
382 conducted in the DISCOL area in 2015 (Greinert, 2015). The freshly created EBS track in the
383 DISCOL area was re-visited 5 weeks after the disturbance experiment, where the surface
384 sediment was mostly removed and deeper sediment layers were exposed without visible
385 sediment mixing (Boetius, 2015; Paul et al., 2018). In a study on the geochemical regeneration
386 in disturbed sediments of the DISCOL area in the Peru Basin, Paul et al. (2018) have shown
387 that the bulk Mn-rich top sediment layer, which has been observed in undisturbed sediments, is
388 removed in the 5-week old EBS disturbance track. Thus, an important pre-requisite for this
389 method is met and the authors have proposed that the depth distribution of solid-phase Mn may
390 be suitable for the evaluation of the impact as well as for the monitoring of the recovery of
391 small-scale disturbance experiments.

392 (2) The fact that the solid-phase Mn maxima in the surface sediments ~~of the CCZ~~ appear to be
393 a regional phenomenon across the CCZ area as it has been observed throughout the different
394 exploration areas (Volz et al., under review)studied in the framework of this study (Volz et al.,
395 in press): The investigated disturbed sediments as well as the undisturbed reference sediments
396 in the CCZ show decreasing solid-phase Mn contents with depth in the upper 20-30 cm of the
397 sediments (Fig. 3; Fig. 4; Volz et al., in press~~under review~~). In the undisturbed reference
398 sediments, solid-phase Mn contents show maxima of up to 1 wt% in the upper 10 cm of the
399 sediments with distinctly decreasing contents below (Fig. 4; Volz et al., in press~~under review~~).
400 Similar bulk solid-phase Mn distribution patterns have been reported for other sites within the
401 CCZ (e.g., Khripounoff et al., 2006; Mewes et al., 2014; Widmann et al., 2014). Volz et al. (in
402 press~~under review~~) have suggested that the widely observed solid-phase Mn enrichments in ~~the~~
403 CCZ surface sediments ~~of the CCZ~~ formed –in association with a more compressed ~~redox~~
404 zonation~~noxic zone~~, which may have prevailed ~~during the last glacial period~~ as a result of lower
405 bottom-water oxygen concentrations during the last glacial period than today. Strong indication

406 for lower glacial bottom-water oxygen concentrations throughout the eastern Pacific Ocean
407 have been provided by a number of independent proxies (e.g., Anderson et al., 2019 and
408 references therein). As a consequence of the ~~is~~ condensed ~~redox zonation~~oxic zone, upward
409 diffusing pore-water Mn²⁺ may have precipitated as authigenic Mn(IV) at a shallow oxic-
410 suboxic redox boundary in the upper few centimeters of the sediments. After the last glacial
411 period, the authigenic Mn(IV) peak was continuously mixed into subsequently deposited
412 sediments by bioturbation causing the observed broad solid-phase Mn(IV) enrichment in the
413 surface sediments (Fig. 4; Volz et al., in press~~under review~~).

414 (3) Lastly, the OPD at all sites is located at sediment depths greater than 0.5 m, and thus,
415 diagenetic precipitation of Mn(IV) in the surface sediments (e.g. Gingele and Kasten, 1994)
416 since the last glacial period can be ruled out (Table 2; Mewes et al., 2014; Volz et al., in
417 ~~press~~under review).

418 Based on the depth distribution of solid-phase Mn, our work suggests that between 5 and 15 cm
419 of the surface sediments were removed and pushed aside by the different small-scale
420 disturbance experiments in the CCZ (Table 3; Fig. 4). This range of disturbance depths is in
421 good agreement with other estimates for small-scale disturbances by similar gear in the CCZ
422 and in the DISCOL area, which suggest that the upper 4-20 cm of the sediments were removed
423 (e.g., Thiel, 2001; Oebius et al., 2001; König et al., 2001; Grupe et al., 2001; Radziejewska,
424 2002; Khrpounoff et al., 2006; Paul et al., 2018). However, as the disturbed sites investigated
425 in this study and the respective undisturbed reference sites are located up to 5 km apart from
426 each other, the correlation of solid-phase Mn may be influenced by some spatial heterogeneities
427 in solid-phase Mn contents (Table 1; Mewes et al., 2014). Furthermore, it should be noted, that
428 for the correlation of solid-phase Mn contents between the disturbed and undisturbed reference
429 sites, we have not considered that (1) particles may have re-settled on the freshly exposed
430 sediment surfaces from re-suspended particle plumes (e.g., Jankowski and Zielke, 2001; Thiel,
431 2001; Radziejewska, 2002; Gillard et al., 2019), (2) sediment has slid off from adjacent flanks
432 of the sediment accumulation after the disturbances (Fig. 2) and (3) sediments have been
433 deposited after the small-scale disturbances at sedimentation rates between 0.2 and 1.2 cm kyr⁻¹
434 (Table 2; Volz et al., 2018). However, only in the case of the IOM-BIE disturbance, the visual
435 impact assessment suggested that the disturbance surface was concealed, here by re-settling
436 sediments (Fig. 2). The development of a re-suspended particle plume during the disturbance
437 experiments highly depends on various factors, such as sediment properties, seafloor
438 topography, bottom-water currents and the disturbance device (e.g., Gillard et al., 2019).

439 Although local and regional variations in these factors have been reported for the CCZ, they
440 are not well constrained (e.g., Mewes et al., 2014; Aleynik et al., 2017; Volz et al., 2018; Gillard
441 et al., 2019; Hauquier et al., ~~under review2019~~). As the disturbance tracks investigated in the
442 framework of this study are relatively small with a maximum width of 2.5 m (Fig. 2; Brockett
443 and Richards, 1994; Brenke 2005), re-suspended particles may (1) only partly deposit on the
444 disturbance track and (2) mostly be transported laterally by currents and deposit on top of
445 undisturbed sediments in the proximity of the disturbance tracks (e.g., Fukushima, 1995;
446 Aleynik et al., 2017; Gillard et al., 2019). This is in accordance with the close correlation of the
447 sediment porosity between the disturbed and undisturbed reference sites, which indicates that
448 the deposition of re-settling particles with higher porosity at the sediment surface in the
449 disturbance tracks is insignificant at all sites, except for the IOM-BIE site (Fig. 4). The porosity
450 data further shows that sediment compaction, potentially caused by the weight of the
451 disturbance device (Cuvelier et al., 2018; Hauquier et al., ~~under review2019~~) is insignificant at
452 all disturbed sites.

453 **4.2. Impact of small-scale disturbances on the geochemical system**

454 The geochemical conditions found at the study sites in the CCZ are the result of a balanced
455 interplay of key factors, such as the input of fresh, labile TOC, sedimentation rate and
456 bioturbation intensity (e.g., Froelich et al., 1979; Berner, 1981; Zonneveld et al., 2010;
457 Mogollón et al., 2016; Volz et al., 2018). Together they characterize the upper reactive layer,
458 which in turn plays a crucial role for the location of the OPD in the sediments of the CCZ (e.g.,
459 Mewes et al., 2014; Mogollón et al., 2016; Volz et al., 2018). Oxygen is consumed via aerobic
460 respiration during the degradation of organic matter while bioturbation transports fresh, labile
461 TOC into deeper sediments (e.g., Haeckel et al., 2001; König et al., 2001). The presence of
462 labile TOC throughout the bioturbated zone significantly enhances the consumption of oxygen
463 with depth, where oxygen is not as easily replenished by seawater oxygen. Thus, the availability
464 of labile TOC in the bioturbated layer controls the amount of oxygen that passes through the
465 reactive layer into deeper sediments (e.g., König et al., 2001). Below the highly reactive layer,
466 refractory organic matter degradation and secondary redox reactions – such as oxidation of
467 Mn^{2+} – control the consumption of oxygen (Supplementary Table 1; Mogollón et al., 2016;
468 Volz et al., 2018). The oxygen profile, more precisely the position of the OPD, in turn, strongly
469 influences the distribution of other solutes. Below the OPD, denitrification and $Mn(IV)$
470 reduction commence, albeit at much lower rates, consuming pore-water NO_3^- and releasing
471 Mn^{2+} (Mogollón et al., 2016; Volz et al., 2018). The study sites in the CCZ provide an excellent
472 example for how slight differences in key environmental factors can profoundly change the

473 overall solute profiles with OPDs ranging between 0.5 m (BGR-RA) and > 7.4 m (GSR) as
474 outlined by Volz et al. (2018).

475 ~~Mining-related~~The removal of the upper 5-15 cm of the sediment results, on one hand, in an
476 almost complete loss of the labile TOC fraction (Fig. 4) as this fraction is restricted to the upper
477 20 cm of the sediment in the CCZ (e.g., Müller and Mangini, 1980; Emerson, 1985; Müller et
478 al., 1988; Mewes et al., 2014; Mogollón et al., 2016; Volz et al., 2018). On the other hand,
479 studies on faunal diversity and density in small-scale disturbances in the sediments of the CCZ
480 and in the DISCOL area show that most of the biota is lost immediately after the disturbance
481 experiment (Borowski et al., 1998; 2001; Bluhm et al., 2001; Thiel et al., 2001; Vanreusel et
482 al., 2016; Jones et al., 2017; Gollner et al., 2017). Thus, a drastic decline or stand-still of
483 bioturbation can be expected in the surface sediments.

484 Based on the results of the transient transport-reaction model, geochemical recovery after small-
485 scale sediment disturbances can be divided into two main phases (Fig. 8):

486 (1) Since the labile TOC fraction and bioturbating fauna is mostly removed, downward
487 diffusion of oxygen is the main driver shaping solute profiles towards a new geochemical
488 ~~equilibrium~~steady state system in the absence of the reactive layer (Figs. 5 and 6). This entails
489 the downward migration of the OPD, as oxygen is no longer effectively consumed in the upper
490 sediment layer. The presence of oxygen outcompetes denitrification and Mn(IV) reduction and
491 induces NH_4^+ and Mn^{2+} oxidation instead, thus, minimizing pore-water NH_4^+ and Mn^{2+}
492 concentrations (Figs. 5 and 6). At the same time, NO_3^- , as a by-product of aerobic-respiration
493 (e.g., Froelich et al., 1979; Berner, 1981; Haeckel et al., 2001; Mogollón et al., 2016; Volz et
494 al., 2018), is accordingly reduced during denitrification and NO_3^- concentrations are lowered
495 during this first phase.

496 (2) The second phase is characterized by the increasing influence of reactive fluxes across the
497 seafloor. It takes approximately 1000 yr before any significant build-up of an upper labile TOC
498 layer is re-established (Fig. 6), at which point solute profiles slowly shift towards their pre-
499 disturbance shape (Fig. 7). Interestingly, during the transition time when oxygen is still present
500 at depth but aerobic respiration in the upper sediments has already began to pick up, NO_3^-
501 concentrations are strongly elevated in the BGR sediments (Figs. 5 and 6). This is due to the
502 fact that NO_3^- is not consumed during denitrification or the Mn-annamox reaction in the
503 presence of oxygen (Mogollón et al., 2016; Volz et al., 2018).

504 With the importance of bioturbation and the mining-related removal of associated fauna in
505 mind, solute and in particular nutrient fluxes across the seafloor should also be considered. The
506 release of nutrients complements the close link between sediment geochemistry and the food
507 web structure (e.g., Smith et al., 1979; Dunlop et al., 2016; Stratmann et al., 2018) and further
508 emphasizes their interdependencies. Figure 7 depicts fluxes of oxygen, NO_3^- and NH_4^+ across
509 the seafloor. As expected, with the reactive layer being mostly absent, fluxes across the seafloor
510 are severely reduced, which particularly affects the oxygen uptake of the sediments as well as
511 the release of NO_3^- and NH_4^+ into the bottom water. At about 100 to 1000 yr after the
512 disturbance, concurrent with the build-up of an upper sediment layer containing significant
513 amounts of labile organic matter, fluxes begin to increase again, albeit much slower than the
514 rate of the decrease in fluxes subsequently after the disturbances (Fig. 7, note the logarithmic
515 scale).

516 It should be noted that while bioturbation has a pivotal influence on the undisturbed steady-
517 state profile, it only plays a secondary role in re-establishing the steady state geochemical
518 equilibrium-system at the disturbed sites in the CCZ. Studies suggest that faunal abundances
519 fully recover within centuries after the disturbance even though the benthic community may be
520 different than prior to the disturbance (e.g., Miljutin et al., 2011; Vanreusel et al., 2016). Due
521 to the extremely slow build-up of the reactive layer with labile TOC, the bioturbation ‘pump’
522 is active again before any significant amount of labile TOC is present about 1-100 kyr after the
523 disturbance. Thus, full recovery is mainly controlled by the re-establishment of the upper
524 reactive layer, i.e. the accumulation rate of labile TOC on the seafloor.

525 The transport-reaction model reveals that under current depositional conditions, the re-
526 equilibratednew steady state geochemical system is established after 1-10 kyr at the IOM-BIE
527 site, while the re-establishment ofthe steady state geochemical conditionequilibrium at the
528 BGR-RA site takes 10-100 kyr (Figs. 5 and 6). Shorter recovery times at the IOM site compared
529 to the BGR-RA site are related to higher sedimentation rates (1.15 instead of 0.65 cm kyr^{-1}) and
530 shallower impact on the sediment (7 cm instead of 10 cm sediment removal). Accordingly, the
531 maximum OPD is reached after 100 yr and 10 kyr at the IOM and BGR-RA site, respectively
532 (Figs. 5 and 6) while the reactive layer is clearly established sooner at the IOM site compared
533 to the BGR-RA site (Fig. 7). Thus, the disturbance depth clearly has a strong influence on the
534 recovery process of the geochemical system of the sediments, highlighting the importance of
535 low-impact mining equipment. Considering that in the CCZ areas of about 8500 km^2 could be
536 commercially mined in 20 yr per individual mining operation (Madureira et al., 2016), this

537 impact assessment of small-scale disturbance experiments may only represent a first approach
538 for the prediction of the environmental impact of large-scale deep-sea mining activities.

539 **5. Conclusion**

540 We have studied surface sediments from seven small-scale disturbance experiments for the
541 simulation of deep-sea mining, which were performed between 1 day and 37 years prior to our
542 sampling in the NE Pacific Ocean. These small-scale disturbance tracks were created using
543 various disturbance devices in different European contract areas for the exploration of
544 polymetallic nodules within the eastern part of the Clarion-Clipperton Zone (CCZ). Through
545 correlation of solid-phase Mn contents of disturbed and undisturbed reference sediments, we
546 (1) propose that the depth distribution of solid-phase Mn in the sediments of the CCZ provides
547 a reliable tool for the estimation of the disturbance depth and (2) show that 5-15 cm of the
548 sediments were removed during the small-scale disturbance experiments investigated in this
549 study. As the small-scale disturbances are associated with the removal of the surface sediments
550 characterized by reactive labile organic matter, the disturbance depth ultimately determines the
551 impact on the geochemical system in the sediments. The application of a transient transport-
552 reaction model reveals that the removal of the upper 7-10 cm of the surface sediments is
553 associated with a meter-scale downward extension of the oxic zone and the shutdown of
554 denitrification and Mn(IV) reduction. As a consequence of lower respiration rates after the
555 disturbance experiments, the geochemical system in the sediments is controlled by downward
556 oxygen diffusion. While the re-establishment of bioturbation within centuries after the
557 disturbance is important for the development of steady state geochemical ~~re~~
558 ~~equilibration conditions~~ in the disturbed sediments, the rate at which ~~the new~~ geochemical
559 steady state system conditions are reached ~~re-equilibrates~~ ultimately depends on the burial rate
560 of organic matter. Assuming the accumulation of labile organic matter to proceed at current
561 Holocene sedimentation rates in the disturbed sediments, biogeochemical reactions resume in
562 the reactive surface sediment layer, and thus, the new steady state geochemical ~~equilibrium~~
563 system in the disturbed sediments in the CCZ is reached on a millennial time scale after the
564 disturbance of the surface sediments.

565 Our study represents the first study on the impact of small-scale disturbance experiments on the
566 sedimentary geochemical system in the prospective areas for polymetallic nodule mining in the
567 CCZ. Our findings on the evaluation of the disturbance depths using solid-phase Mn contents
568 as well as the quantification of the development of a new geochemical ~~re-equilibration~~
569 steady state system – in the sediments advances our knowledge about the potential long-term

570 consequences of deep-sea mining activities. We propose that mining techniques potentially
571 used for the potential commercial exploitation of nodules in the CCZ may remove less than
572 10 cm of the surface sediments in order to minimize the impact on the geochemical system in
573 the sediments. The depth distribution of solid-phase Mn may be used for environmental
574 monitoring purposes during future mining activities in the CCZ. However, based on our current
575 knowledge and in combination with ongoing natural environmental changes (e.g., bottom water
576 warming, acidification, changes in the POC flux to the seafloor), it is difficult to assess whether
577 the surface sediment removal may trigger a tipping point for deep-sea ecosystems. Furthermore,
578 the depth distribution of solid phase Mn may be used for environmental monitoring purposes
579 during future mining activities in the CCZ. This study also provides valuable data for further
580 investigations on the environmental impact of deep-sea mining, such as during the launched JPI
581 Oceans follow-up project MiningImpact 2.

582 **Data availability**

583 The data are available via the data management portal OSIS-Kiel and the WDC database
584 PANGAEA, including the solid-phase bulk sediment Mn and TOC contents
585 (<https://doi.org/10.1594/PANGAEA.904560>) as well as the porosity data
586 (<https://doi.org/10.1594/PANGAEA.904578>).

587 **Author contribution**

588 The study was conceived by all co-authors. JBV carried out the sampling and analyses on board
589 during RV SONNE cruise SO239 and the analytical work in the laboratories at AWI in
590 Bremerhaven. LH and MH modified the numerical transport-reaction model presented in Volz
591 et al. (2018) and provided model results for the long-term effects of small-scale disturbances
592 on geochemical conditions and biogeochemical processes. JBV prepared the manuscript with
593 substantial contributions from all co-authors.

594 **Competing interest**

595 The authors declare that they have no conflict of interest.

596 **Acknowledgements**

597 We thank captain Lutz Mallon, the crew and the scientific party of RV SONNE cruise SO239
598 for the technical and scientific support. Thanks to Jennifer Ciomber, Benjamin Löffler and
599 Vincent Ozegowski for their participation in sampling and analysis onboard. For analytical

600 support in the home laboratory and during data evaluation we are grateful to Ingrid Stimac, Olaf
601 Kreft, Dennis Köhler, Ingrid Dohrmann (all at AWI). Special thanks to Prof. Dr. Gerhard
602 Bohrmann (MARUM, University of Bremen), Dr. Timothy G. Ferdelman (MPI Bremen) and
603 Dr. Ellen Pape (University of Ghent) for much appreciated discussions.

604 This study is funded by the Bundesministerium für Bildung und Forschung (BMBF Grant
605 03F0707A+G) as part of the JPI-Oceans pilot action “Ecological Aspects of Deep-Sea Mining
606 (MiningImpact)”. We acknowledge further financial support from the Helmholtz Association
607 (Alfred Wegener Institute Helmholtz Centre for Polar and Marine Research).

608 **References**

609 Aleynik, D., Inall, M. E., Dale, A., and Vink, A.: Impact of remotely generated eddies on plume
610 dispersion at abyssal mining sites in the Pacific, *Sci. Rep.*, 7, 1–14, doi:10.1038/s41598-
611 017-16912-2, 2017.

612 [Anderson, R.F., Sachs, J.P., Fleisher, M.Q., Allen, K.A., Yu, J., Koutavas, A., and Jaccard, S.L.](#)
613 [Deep-sea oxygen depletion and ocean carbon sequestration during the last ice age. Global](#)
614 [Biogeochem. Cycles, 33, 301-317, doi:10.1029/2018GB006049, 2019.](#)

615 Berger, W. H.: Deep-sea sedimentation, in: *The Geology of Continental Margins*, edited by:
616 Burk, C. A., and Drake, C. L., Springer, New York, 213–241, 1974.

617 Berner, R. A.: A new geochemical classification of sedimentary environments, *J. Sediment.*
618 *Petrol.*, 51, 359-365, 1981.

619 Berner, R. A.: *Early Diagenesis: A Theoretical Approach*, Princeton University Press,
620 Princeton, 1-24, 1980.

621 Bluhm H.: Re-establishment of an abyssal megabenthic community after experimental physical
622 disturbance of the seafloor, *Deep-Sea Res. Part II Top. Stud. Oceanogr.*, 48, 3841–3868,
623 2001.

624 Boetius, A., and Haeckel, M.: Mind the seafloor, *Science*, 359, 34-36,
625 doi:10.1126/science.aap7301, 2018.

626 Boetius, A.: *RV Sonne Fahrtbericht / Cruise Report SO242-2: JPI OCEANS Ecological*
627 *Aspects of Deep-Sea Mining, DISCOL Revisited, Guayaquil-Guayaquil (Ecuador), 28.08.-*
628 *01.10.2015*, Kiel: Helmholtz-Zentrum für Ozeanforschung, 2015.

629 Borowski, C.: Physically disturbed deep-sea macrofaunal impacts of a large-scale physical
630 disturbance experiment in the Southeast Pacific, *Deep-Sea Res. Part II Top. Stud.*
631 *Oceanogr.*, 48, 3809–3839, 2001.

632 Borowski, C., and Thiel, H.: Deep-Sea macrofaunal impacts of a large-scale physical
633 disturbance experiment in the Southeast Pacific, *Deep-Sea Res. Part II Top. Stud.*
634 *Oceanogr.*, 45, 55-81, 1998.

635 Boudreau, B. P.: A one-dimensional model for bed-boundary layer particle exchange, *J. Mar.*
636 *Syst.*, 11, 279–303, doi:10.1016/S0924-7963(96)00127-3, 1997.

637 Brenke, N.: An Epibenthic sledge for operations on marine soft bottom and bedrock, *J. Mar.*
638 *Tech. Soc.*, 39, 10–19, 2005.

639 Brockett, T., and Richards, C. Z.: Deep-sea mining simulator for environmental impact studies,
640 *Sea Technol.*, 35, 77-82, 1994.

641 Chung, J. S.: Full-Scale, Coupled Ship and Pipe Motions Measured in North Pacific Ocean:
642 The Hughes Glomar Explorer with a 5,000-m-Long Heavy-Lift Pipe Deployed, *Proc. 19th*
643 *ISOPE*, 20, 1-6, 2010.

644 Cronan, D. S., Rothwell, G., and Croudace, I.: An ITRAX geochemical study of
645 ferromanganeseous sediments from the Penrhyn basin, South Pacific Ocean, *Mar.*
646 *Georesour. Geotechnol.*, 28, 207–221, doi:10.1080/1064119X.2010.483001, 2010.

647 Cuvelier, D., Gollner, S., Jones, D. O. B., Kaiser, S., Arbizu, P. M., Menzel, L., Mestre, N. C.,
648 Morato, T., Pham, C., Pradillon, F., Purser, A., Raschka, U., Sarrazin, J., Simon-Lledó, E.,
649 Stewart, I.M., Stuckas, H., Sweetman, A. K., and Colaço, A.: Potential Mitigation and
650 Restoration Actions in Ecosystems Impacted by Seabed Mining, *Front. Mar. Sci.*, 5,
651 doi:10.3389/fmars.2018.00467, 2018.

652 Davies, A. J., Roberts, J. M., and Hall-Spencer, J.: Preserving deep-sea natural heritage:
653 emerging issues in offshore conservation and management, *Biol. Conserv.*, 138, 299–312,
654 doi:10.1016/j.biocon.2007.05.011, 2007.

655 Dunlop, K. M., van Oevelen, D., Ruhl, H. A., Huffard, C. L., Kuhnz, L. A., and Smith, K. L.:
656 Carbon cycling in the deep eastern North Pacific benthic food web: Investigating the effect

657 of organic carbon input, Limnol. Oceanogr., 61, 1956–1968,
658 <https://doi.org/10.1002/lno.10345>, 2016.

659 Emerson, S., Fischer, K., Reimers, C. and Heggie, D.: Organic carbon dynamics and
660 preservation in deep-sea sediments, Deep-Sea Res., 32, 1–21, 1985.

661 Froelich, P. N., Klinkhammer, G. P., Bender, M. L., Luedke, L. A., Heath, G. R., Cullen, C.,
662 Dauphin, P., Hammond, D., Hartmann, B., and Maynard, V.: Early oxidation of organic
663 matter in pelagic sediments of the Eastern Equatorial Pacific, suboxic diagenesis, Geochim.
664 Cosmochim. Acta, 43, 1075–1090, 1979.

665 Fukushima, T.: Overview "Japan Deep-Sea Impact Experiment = JET", ISOPE-M-95-008,
666 ISOPE, 1995.

667 Gillard, B., Purkiani, K., Chatzivangelou, D., Vink, A., Iversen, M. H., and Thomsen, L.:
668 Physical and hydrodynamic properties of deep sea mining-generated, abyssal sediment
669 plumes in the Clarion Clipperton Fracture Zone (eastern-central Pacific), Elem. Sci. Anth.,
670 7, 2019.

671 Gingele, F. X., and Kasten, S.: Solid-phase manganese in Southeast Atlantic sediments:
672 implications for the paleoenvironment. Mar. Geol., 121, 317–332, 1994.

673 Glasby, G. P.: Lessons Learned from Deep-Sea Mining. Science, 289, 551–553,
674 doi:10.1126/science.289.5479.551, 2000.

675 Glover, A. G. and Smith, C. R.: The deep-sea floor ecosystem: current status and prospects of
676 anthropogenic change by the year 2025, Environ. Conserv., 30, 219–241, 2003.

677 Gollner, S., Kaiser, S., Menzel, L., Jones, D. O. B., Brown, A., Mestre, N. C., van Oevelen, D.,
678 Menot, L., Colaço, A., Canals, M., Cuvelier, D., Durden, J. M., Gebruk, A., Egho, G. A.,
679 Haeckel, M., Marcon, Y., Mevenkamp, L., Morato, T., Pham, C. K., Purser, A., Sanchez-
680 Vidal, A., Vanreusel, A., Vink, A., and Arbizu, P. M.: Resilience of benthic deep-sea fauna
681 to mining activities, Mar. Environ. Res., 129, 76–101,
682 doi:10.1016/j.marenvres.2017.04.010. 2017.

683 Greinert, J.: RV Sonne Fahrbericht / Cruise Report SO242-1: JPI OCEANS Ecological Aspects
684 of Deep-Sea Mining, DISCOL Revisited, Guayaquil-Guayaquil (Ecuador), 28.07.–
685 25.08.2015, Kiel: Helmholtz-Zentrum für Ozeanforschung, 2015.

686 Grupe, B., Becker, H. J., and Oebius, H. U.: Geotechnical and sedimentological investigations
687 of deep-sea sediments from a manganese nodule field of the Peru Basin, Deep. Res. Part II
688 Top. Stud. Oceanogr., 48, 3593–3608, 2001.

689 Haeckel, M., König, I., Riech, V., Weber, M. E., and Suess, E.: Pore water profiles and
690 numerical modelling of biogeochemical processes in Peru Basin deep-sea sediments, Deep.
691 Res. Part II Top. Stud. Oceanogr., 48, 3713–3736, doi:10.1016/S0967-0645(01)00064-9,
692 2001.

693 Hauquier, F., Macheriotou, L., Bezerra, T. N., Egho, G., Martínez Arbizu, P., and Vanreusel,
694 A.: Geographic distribution of free-living marine nematodes in the Clarion-Clipperton
695 Zone: implications for future deep-sea mining scenarios, Biogeosciences, [16\(18\)Discusses. 3475-3489.](https://doi.org/10.5194/bg-16-3475-2019) <https://doi.org/10.5194/bg-16-3475-2019> [10.5194/bg-2018-492](https://doi.org/10.5194/bg-2018-492), under review,
696 20182019.

697 Halfar, J., and Fujita, R. M.: Precautionary management of deep-sea mining, Mar. Pol., 26, 103–
698 106, 2002.

699 Halkyard, J. E.: Technology for Mining Cobalt Rich Manganese Crusts from Seamounts, Proc.
700 OCEANS '85, 352–274, 1985.

701 Halbach, P., Friedrich, G., and von Stackelberg, U. (Eds.): The manganese nodule belt of the
702 Pacific Ocean, Enke, Stuttgart, 1988.

703 Hein, J. R., Mizell, K., Koschinsky, A., and Conrad, T. A.: Deep-ocean mineral deposits as a
704 source of critical metals for high- and green-technology applications: comparison with
705 land-based resources, Ore Geol. Rev., 51, 1–14, 2013.

707 Hoagland, P., Beaulieu, S., Tivey, M. A., Eggert, R. G., German, C., Glowka, L., and Lin, J.:
708 Deep-sea mining of seafloor massive sulfides, *Mar. Pol.*, 34, 728-732,
709 doi:10.1016/j.marpol.2009.12.001, 2010.

710 International Seabed Authority (ISA): A Geological Model for Polymetallic Nodule Deposits
711 in the Clarion-Clipperton Fracture Zone, Technical Study 6, Kingston, p. 211, 2010.

712 Jankowski, J. A., and Zielke, W.: The mesoscale sediment transport due to technical activities
713 in the deep sea, *Deep. Res. Part II Top. Stud. Oceanogr.*, 48, 3487–3521, 2001.

714 Jones, D. O. B., Kaiser, S., Sweetman, A. K., Smith, C. R., Menot, L., Vink, A., Trueblood, D.,
715 Greinert, J., Billett, D. S. M., Martínez Arbizu, P., Radziejewska, T., Singh, R., Ingole, B.,
716 Stratmann, T., Simon-Lledó, E., Durden, J. M., and Clark, M. R.: Biological responses to
717 disturbance from simulated deep-sea polymetallic nodule mining, *PLoS One*, 12,
718 e0171750, <https://doi.org/10.1371/journal.pone.0171750>, 2017.

719 Juan, C., Van Rooij, D., and De Bruycker, W.: An assessment of bottom current controlled
720 sedimentation in Pacific Ocean abyssal environments, *Mar. Geol.*, 403, 20–33, 2018.

721 Khrpounoff, A., Caprais, J.-C., Crassous, P. and Etoubleau, J.: Geochemical and biological
722 recovery of the disturbed seafloor in polymetallic nodule fields of the Clipperton-Clarion
723 Fracture Zone (CCFZ) at 5,000-m depth, *Limnol. Oceanogr.*, 51, 2033–2041,
724 doi:10.4319/lo.2006.51.5.2033, 2006.

725 König, I., Haeckel, M., Lougear, A., Suess, E., and Trautwein, A. X.: A geochemical model of
726 the Peru Basin deep-sea floor - and the response of the system to technical impacts, *Deep.*
727 *Res. Part II Top. Stud. Oceanogr.*, 48, 3737–3756, doi:10.1016/S0967-0645(01)00065-0,
728 2001.

729 Kotlinski R, and Stoyanova V.: Physical, Chemical, and Geological changes of Marine
730 Environment Caused by the Benthic Impact Experiment at the IOM BIE Site, *Proc. 8th*
731 *ISOPE 2*, 277-281, Montreal, Canada, 1998.

732 Kretschmer, S., Geibert, W., Rutgers van der Loeff, M. M., and Mollenhauer, G.: Grain size
733 effects on 230Thxs inventories in opal-rich and carbonate-rich marine sediments, *Earth*
734 *Planet. Sci. Lett.*, 294, 131–142, doi:10.1016/j.epsl.2010.03.021, 2010.

735 Kuhn, G.: Don't forget the salty soup: Calculations for bulk marine geochemistry and
736 radionuclide geochronology, *Goldschmidt 2013* Florence, Italy, 25 August 2013 - 30
737 August 2013, doi:10.1180/minmag.2013.077.5.11, 2013.

738 Kuhn, T., Wegorzewski, A. V., Rühlemann, C., and Vink, A.: Composition, formation, and
739 occurrence of polymetallic nodules, in: *Deep-Sea Mining*, edited by: Sharma, R., 23–63,
740 Springer International Publishing, Cham., doi:10.1007/978-3-319-52557-0_2, 2017a.

741 Kuhn, T., Versteegh, G. J. M., Villinger, H., Dohrmann, I., Heller, C., Koschinsky, A., Kaul,
742 N., Ritter, S., Wegorzewski, A. V. and Kasten, S.: Widespread seawater circulation in 18–
743 22 Ma oceanic crust: Impact on heat flow and sediment geochemistry, *Geology*, 45, 799–
744 802, doi:10.1130/G39091.1, 2017b.

745 Kuhn, T., Rühlemann, C., and Wiedicke-Hombach, M.: Developing a strategy for the
746 exploration of vast seafloor areas for prospective manganese nodule fields, in: *Marine*
747 *Minerals: Finding the Right Balance of Sustainable Development and Environmental*
748 *Protection*, edited by Zhou, H., and Morgan, C. L., The Underwater Mining Institute,
749 Gelendzhik, Russia (K 1-12), 2012.

750 Lodge, M., Johnson, D., Le Gurun, G., Wengler, M., Weaver, P., and Gunn, V.: Seabed mining:
751 International Seabed Authority environmental management plan for the Clarion–
752 Clipperton Zone. A partnership approach, *Mar. Pol.*, 49, 66–72,
753 doi:10.1016/j.marpol.2014.04.006, 2014.

754 Madureira, P., Brekke, H., Cherkashov, G., and Rovere, M.: Exploration of polymetallic
755 nodules in the Area: Reporting practices, data management and transparency, *Mar. Pol.*,
756 70, 101–107, doi:10.1016/j.marpol.2016.04.051, 2016.

757 Martínez Arbizu, P., and Haeckel, M.: RV SONNE Fahrbericht / Cruise Report SO239:
758 EcoResponse Assessing the Ecology, Connectivity and Resilience of Polymetallic Nodule
759 Field Systems, Balboa (Panama) – Manzanillo (Mexico,) 11.03.-30.04.2015 (Report No.
760 doi:10.3289/GEOMAR REP_NS_25_2015), GEOMAR Helmholtz-Zentrum für
761 Ozeanforschung, Kiel, Germany, 2015.

762 Menendez, A., James, R. H., Lichtschlag, A., Connelly, D. and Peel, K.: Controls on the
763 chemical composition on ferromanganese nodules in the Clarion-Clipperton Fracture Zone,
764 eastern equatorial Pacific, *Mar. Geol.*, 409, 1-14, 2018.

765 Menot, L., and Rühlemann, C., and BIONOD Shipboard party: BIONOD Cruise Science
766 Report, Vol. 2 French Licence Area, Ifremer, REM/EEP/LEP13.06, 57p, 2013.

767 Mero, J. L.: The Mineral Resources of the Sea, Elsevier, Amsterdam, 1965.

768 Mewes, K., Mogollón, J. M., Picard, A., Rühlemann, C., Eisenhauer, A., Kuhn, T., Ziebis, W.,
769 and Kasten, S.: Diffusive transfer of oxygen from seamount basaltic crust into overlying
770 sediments: An example from the Clarion-Clipperton Fracture Zone, *Earth Planet. Sci.*
771 *Lett.*, 433, 215–225, doi:10.1016/j.epsl.2015.10.028, 2016.

772 Mewes, K., Mogollón, J. M., Picard, A., Rühlemann, C., Kuhn, T., Nöthen, K., and Kasten, S.:
773 Impact of depositional and biogeochemical processes on small scale variations in nodule
774 abundance in the Clarion-Clipperton Fracture Zone, *Deep-Sea Res. Part I: Oceanogr. Res.*
775 *Pap.*, 91, 125–141, doi:10.1016/j.dsr.2014.06.001, 2014.

776 Miljutin, D. M., Miljutina, M. A., Martínez Arbizu, P., and Galeron, J.: Deep-sea nematode
777 assemblage has not recovered 26 years after experimental mining of polymetallic nodules
778 (CCFZ, Pacific), *Deep-Sea Res. Part I: Oceanogr. Res. Pap.*, 58, 885–897, 2011.

779 Mogollón, J. M., Mewes, K., and Kasten, S.: Quantifying manganese and nitrogen cycle
780 coupling in manganese-rich, organic carbon-starved marine sediments: Examples from the
781 Clarion-Clipperton fracture zone, *Geophys. Res. Lett.*, 43, 2016GL069117,
782 doi:10.1002/2016GL069117, 2016.

783 Morgan, C. L., Nichols, J. A., Selk, B. W., Toth, J. R., and Wallin, C.: Preliminary analysis of
784 exploration data from Pacific deposits of manganese nodules, *Mar. Georesour.*
785 *Geotechnol.*, 11, 1-25, 1993.

786 Müller, P. J., Hartmann, M., and Suess, E.: The chemical environment of pelagic sediments, in:
787 The Manganese Nodule Belt of the Pacific Ocean: Geological Environment, Nodule
788 Formation, and Mining Aspects, edited by Halbach, P., Friedrich, G., and von Stackelberg,
789 U., Enke, Stuttgart, pp. 70-90, 1988.

790 Müller, P. J., and Mangini, A.: Organic carbon decomposition rates in sediments of the pacific
791 manganese nodule belt dated by ^{230}Th and ^{231}Pa , *Earth Planet. Sci. Lett.*, 51, 94-114,
792 1980.

793 Nöthen, K., and Kasten, S.: Reconstructing changes in seep activity by means of pore water and
794 solid phase Sr/Ca and Mg/Ca ratios in pockmark sediments of the Northern Congo Fan,
795 *Mar. Geol.*, 287, 1–13, doi:10.1016/j.margeo.2011.06.008, 2011.

796 Oebius, H. U., Becker, H. J., Rolinski, S., and Jankowski, J. A.: Parametrization and evaluation
797 of marine environmental impacts produced by deep-sea manganese nodule mining, *Deep-*
798 *Sea Res. Part II Top. Stud. Oceanogr.*, 48, 3453–3467, doi:10.1016/S0967-
799 0645(01)00052-2, 2001.

800 Paul, S. A. L., Gaye, B., Haeckel, M., Kasten, S., and Koschinsky, A.: Biogeochemical
801 Regeneration of a Nodule Mining Disturbance Site: Trace Metals, DOC and Amino Acids
802 in Deep-Sea Sediments and Pore Waters, *Front. Mar. Sci.*, 5, doi:
803 10.3389/fmars.2018.00117, 2018.

804 Pearson, K.: Notes on regression and inheritance in the case of two parents, *Proc. Royal Soc.*
805 *London*, 58, 240–242, 1895.

806 Purser, A., Marcon, Y., Hoving, H.-J. T., Vecchione, M., Piatkowski, U., Eason, D., Bluhm,
807 H., and Boetius, A.: Association of deep-sea incirrate octopods with manganese crusts and

808 nodule fields in the Pacific Ocean, *Curr. Biol.*, 26, R1268–R1269,
809 doi:10.1016/j.cub.2016.10.052, 2016, 2016.

810 Radziejewska, T.: Response of deep-sea meiobenthic communities to sediment disturbance
811 simulating effects of polymetallic nodule mining, *Int. Rev. Hydrobiol.*, 87, 457–477, 2002.

812 Ramirez-Llodra E., Tyler P. A., Baker M. C., Bergstad O. A., Clark M. R., Escobar, E., Levin,
813 L. A., Menot, L., Rowden, A. A., Smith, C. R., and Van Dover, C. L.: Man and the Last
814 Great Wilderness: Human Impact on the Deep Sea, *PLoS ONE*, 6, e22588,
815 doi:10.1371/journal.pone.0022588, 2011.

816 Redfield, A. C.: On the proportions of organic derivations in sea water and their relation to the
817 composition of plankton, in: *James Johnstone Memorial Volume*, edited by Daniel, R. J.,
818 University Press of Liverpool, pp. 176–192, 1934.

819 Rühlemann, C., Kuhn, T., Wiedicke, M., Kasten, S., Mewes, K., and Picard, A.: Current status
820 of manganese nodule exploration in the German license area, *Proceedings of the Ninth*
821 (2011) ISOPE Ocean Mining Symposium, Maui, Hawaii, USA, June 19-24, 2011, 168–
822 173, 2011.

823 Rühlemann, C., Albers, L., Briand, P., Brulport, J.-P., Cosson, R., Dekov, V. M., Galéron, J.,
824 Goergens, R., Gueguen, B., Hansen, J., Kaiser, S., Kefel, O., Khrpounoff, A., Kuhn, T.,
825 Larsen, K., Menot, L., Mewes, K., Miljutin, D., Mohrbeck, I., Nealova, L., Perret-Gentil,
826 L., Regocheva, A., Wegorzewski, A., and Zoch, D., BIONOD Cruise report, p. 299, 2012.

827 Scott, S. D.: Seafloor Polymetallic Sulfides: Scientific Curiosities or Mines of the Future? In:
828 *Marine Minerals*, edited by: Teleki, P. G., Dobson, M. R., Moore, J. R., and von
829 Stackelberg, U., *NATO ASI Series (Series C: Mathematical and Physical Sciences)*, 194,
830 Springer, Dordrecht, 1987.

831 Sharma, R.: Indian Deep-sea Environment Experiment (INDEX):: An appraisal. *Deep-Sea Res.*
832 Part II Top. Stud. Oceanogr., 48, 3295–3307, doi:10.1016/S0967-0645(01)00041-8, 2001.

833 Smith, C. R., Levin, L. A., Koslow, A., Tyler, P. A., and Glover, A. G.: The near future of the
834 deep seafloor ecosystems, in: *Aquatic Ecosystems: Trends and Global Prospects*, edited by
835 Polunin, N. V. C., Cambridge University Press, 334–353, doi:
836 10.1017/CBO9780511751790.030, 2008.

837 Smith, K. L., White, G. A., and Laver, M. B.: Oxygen uptake and nutrient exchange of
838 sediments measured in situ using a free vehicle grab respirometer. *Deep Sea Res. Part II*,
839 26, 337–346, doi:10.1016/0198-0149(79)90030-X, 1979.

840 Soetaert, K., and Meysman, F.: Reactive transport in aquatic ecosystems: Rapid model
841 prototyping in the open source software R, *Environ. Model. Softw.*, 32, 49–60,
842 doi:10.1016/j.envsoft.2011.08.011, 2012.

843 Spickermann, R.: Rare Earth Content of Manganese Nodules in the Lockheed Martin Clarion-
844 Clipperton Zone Exploration Areas, *Proc. Off. Technol. Conf.*, Houston Texas, 2012.

845 Stratmann, T., Lins, L., Purser, A., Marcon, Y., Rodrigues, C. F., Ravara, A., Cunha, M. R.,
846 Simon-Lledó, E., Jones, D. O. B., Sweetman, A. K., Köser, K., and van Oevelen, D.:
847 Abyssal plain faunal carbon flows remain depressed 26 years after a simulated deep-sea
848 mining disturbance, *Biogeosciences*, 15, 4131–4145, doi.org/10.5194/bg-15-4131-2018,
849 2018.

850 Thiel, H., and Forschungsverband Tiefsee-Umweltschutz: Evaluation of the environmental
851 consequences of polymetallic nodule mining based on the results of the TUSCH Research
852 Association, *Deep-Sea Res. Part II Top. Stud. Oceanogr.*, 48, 3433–3452,
853 doi:10.1016/S0967-0645(01)00051-0, 2001.

854 Trueblood, D. D., and Ozturgut, E.: The benthic impact experiment: A study of the ecological
855 impacts of deep seabed mining on abyssal benthic communities, *Proc. of the 7th ISOPE*
856 Conference, Honolulu, Hawaii, 1997.

857 Van Dover, C. L.: Tighten regulations on deep-sea mining, *Nature*, 470, 31–33, doi:
858 10.1038/470031a, 2011.

859 Vanreusel, A., Hilario, A., Ribeiro, P. A., Menot, L., and Arbizu, P. M.: Threatened by mining,
860 polymetallic nodules are required to preserve abyssal epifauna, *Sci. Rep.*, 6, 26808,
861 doi:10.1038/srep26808, 2016.

862 Volz, J. B., Liu, B., Köster, M., Henkel, S., Koschinsky, A., and Kasten, S.: Post-depositional
863 manganese mobilization during the last glacial period in sediments of the eastern Clarion-
864 Clipperton Zone, Pacific Ocean, *Earth Planet. Sci. Lett.*, [doi:10.1016/j.epsl.2019.116012](https://doi.org/10.1016/j.epsl.2019.116012),
865 [in press, 2019 under review](#).

866 Volz, J. B., Mogollón, J. M., Geibert, W., Martínez Arbizu, P., Koschinsky, A., Kasten, S.:
867 Natural spatial variability of depositional conditions, biogeochemical processes and
868 element fluxes in sediments of the eastern Clarion-Clipperton Zone, Pacific Ocean, *Deep-
869 Sea Res. Part I*, 140, 159-172, 2018.

870 Wedding, L. M., Reiter, S. M., Smith, C. R., Gjerde, K. M., Kittinger, J. N., Friedlander, A. M.,
871 Gaines, S. D., Clark, M. R., Thurnherr, A. M., Hardy, S. M., and Crowder, L. B.: Managing
872 mining of the deep seabed, *Science*, 349, 144-145, 2015.

873 Widmann, P.: Enrichment of mobilizable manganese in relation to manganese nodules
874 abundance, Master thesis, Eberhard Karls Universität Tübingen and the Federal Institute for
875 Geoscience and Resources, Hannover, 182 p., 2015.

876 Ziebis, W., McManus, J., Fertelman, T., Schmidt-Schierhorn, F., Bach, W., Muratli, J.,
877 Edwards, K. J., and Villinger, H.: Interstitial fluid chemistry of sediments underlying the
878 North Atlantic gyre and the influence of subsurface fluid flow, *Earth Planet. Sci. Lett.*,
879 323-324, 79-91, doi:10.1016/j.epsl.2012.01.018, 2012.

880 Zonneveld, K., Versteegh, G., Kasten, S., Eglington, T. I., Emeis, K.-C., Huguet, C., Koch, B.
881 P., de Lange, G. J., de Leeuw, J. W., Middelburg, J. J., Mollenhauer, G., Prahl, F.,
882 Rethemeyer, J. and Wakeham, S.: Selective preservation of organic matter in marine
883 environments; processes and impact on the sedimentary record, *Biogeosciences*, 7, 483-
884 511, 2010.

885

886

887 **Figure captions**

888 Figure 1: Sampling sites (black circles, black star) in various European contract areas for the
889 exploration of manganese nodules within the Clarion-Clipperton Fracture Zone (CCZ).
890 Investigated stations are located in the German BGR area (blue), eastern European IOM area
891 (yellow), Belgian GSR area (green) and French IFREMER area (red). The two stations within
892 the German BGR area are located in the “prospective area” (BGR-PA, black star) and in the
893 “reference area” (BGR-RA, black circle). The contract areas granted/governed by the
894 International Seabed Authority (ISA; white areas) are surrounded by nine Areas of Particular
895 Environmental Interest (APEI), which are excluded from any mining activities (green shaded
896 squares). Geographical data provided by the ISA.

897 Figure 2: Examples of undisturbed reference sediments in the German BGR-PA area and the
898 French IFREMER area and pictures of small-scale disturbances for the simulation of deep-sea
899 mining within the CCZ, which are investigated in the framework of this study (years: yr;
900 months: mth; days: d). Copyright: ROV KIEL 6000 Team, GEOMAR Helmholtz Centre for
901 Ocean Research Kiel, Germany.

902 Figure 3: Solid-phase Mn and TOC contents for all disturbed sites investigated in the framework
903 of this study.

904 Figure 4: Correlation of solid-phase Mn and TOC contents between the disturbed sites and the
905 respective undisturbed reference sediments (grey shaded profiles) using the disturbance depths
906 determined with the Pearson correlation coefficient (compare Table 3). For the undisturbed
907 reference sediments, solid-phase Mn contents are taken from Volz et al. (in press/under review)
908 and TOC contents are taken from Volz et al. (2018).

909 Figure 5: Model results of the transient transport-reaction model for (a) the EBS disturbance in
910 the German BGR-RA area and (b) the IOM-BIE disturbance in the eastern European IOM area.
911 The model is adapted after the steady state transport-reaction model presented in Volz et al.
912 (2018) and shows the response of the geochemical system in the sediments if steady state
913 conditions are disturbed by the removal of the upper 10 cm (BGR-RA, average disturbance
914 depth of BGR-PA and BGR-RA; cf. Table 3) and 7 cm (IOM; Table 3) of the sediments while
915 maintaining the same boundary conditions but with reduced bioturbation over the first 100 years
916 after the disturbance. transient transport-reaction model for (a) EBS disturbance in the German
917 BGR-RA area and (b) the IOM-BIE disturbance in the eastern European IOM area.

918 Figure 6: Detailed model results of the transient transport-reaction model (Figure 5) for the
919 upper 1 m of the sediments with the fit of the simulated profiles with the analytical data for
920 undisturbed sediments at current steady state geochemical conditions and for the new steady
921 state geochemical system after the disturbance (dark blue profiles) for (a) EBS disturbance in
922 the German BGR-RA area and (b) the IOM-BIE disturbance in the eastern European IOM area.

923 Figure 7: Pore-water fluxes of oxygen (O_2), nitrate (NO_3^{2-}) and ammonia (NH_4^+) at the
924 sediment-water interface obtained by the application of the transient transport-reaction model.
925 Oxygen fluxes into the sediment and fluxes of nitrate and ammonia towards the sediment

926 surface are shown as a function of time after the EBS and IOM-BIE disturbances in the German
927 BGR-RA area (blue) and in the eastern European IOM area (black), respectively.

928 Figure 8: Conceptual model for time-dependent pore-water fluxes of oxygen (O_2), nitrate
929 (NO_3^{2-}) and ammonia (NH_4^+) at the sediment-water interface after the removal of the upper 7-
930 10 cm of the sediments. The re-establishment of bioturbation, the maximum oxygen penetration
931 depth (OPD) as well as the re-establishment of the surface sediment layer dominated by the
932 reactive labile organic matter fraction are indicated as a function of time after the sediment
933 removal.

934 **Table captions**

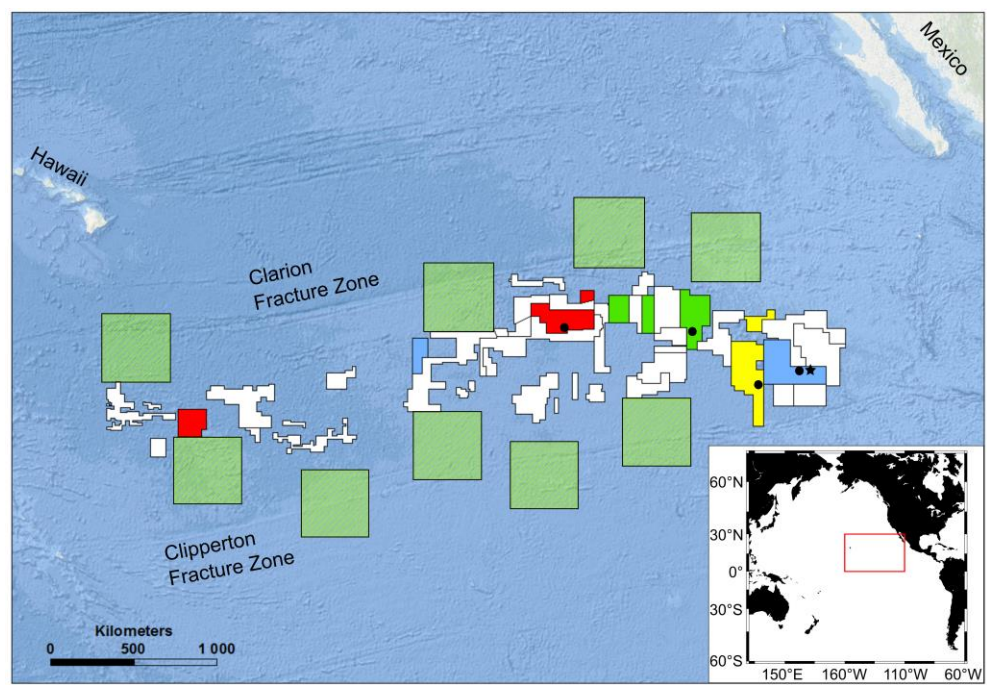
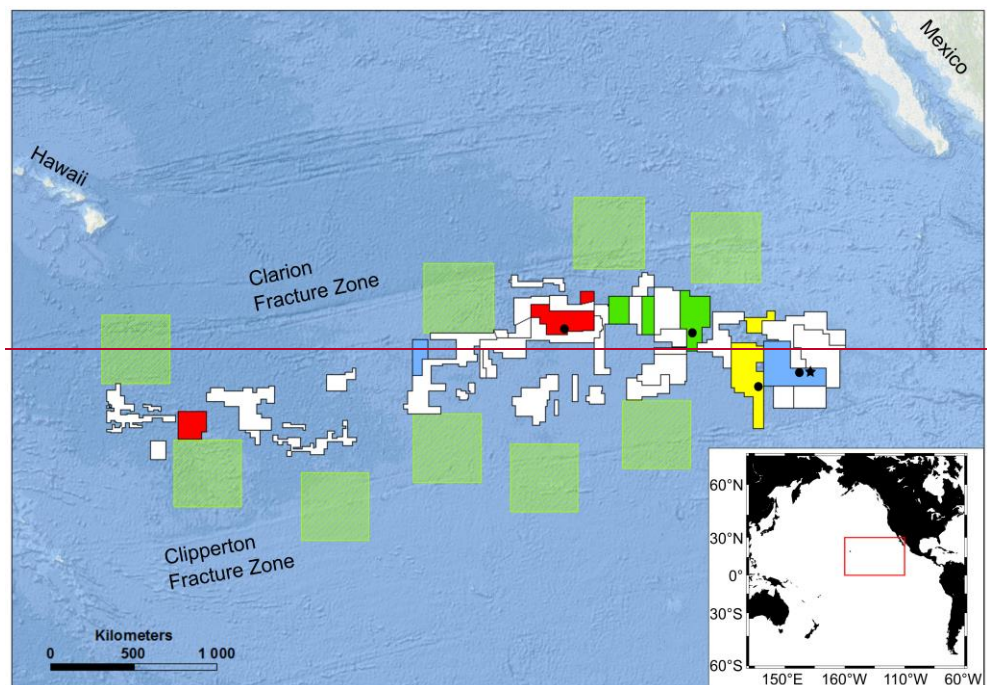
935 Table 1: MUC and PC cores investigated in this study including information on geographic
936 position, water depth, type and age of the disturbances (years: yr; months: mth; days: d).

937 Table 2: Information of sedimentation rate (Sed. rate), flux of particulate organic carbon (POC)
938 to the seafloor, bioturbation depth (Bioturb. depth), oxygen penetration depth (OPD) based on
939 GC cores from the investigated sites and determined in the study by Volz et al. (2018).
940 Information for the BGR-PA area is taken from an adjacent site (A5-2-SN; 11°57.22'N,
941 117°0.42'W) studied by Mewes et al. (2014) and Mogollón et al. (2016).

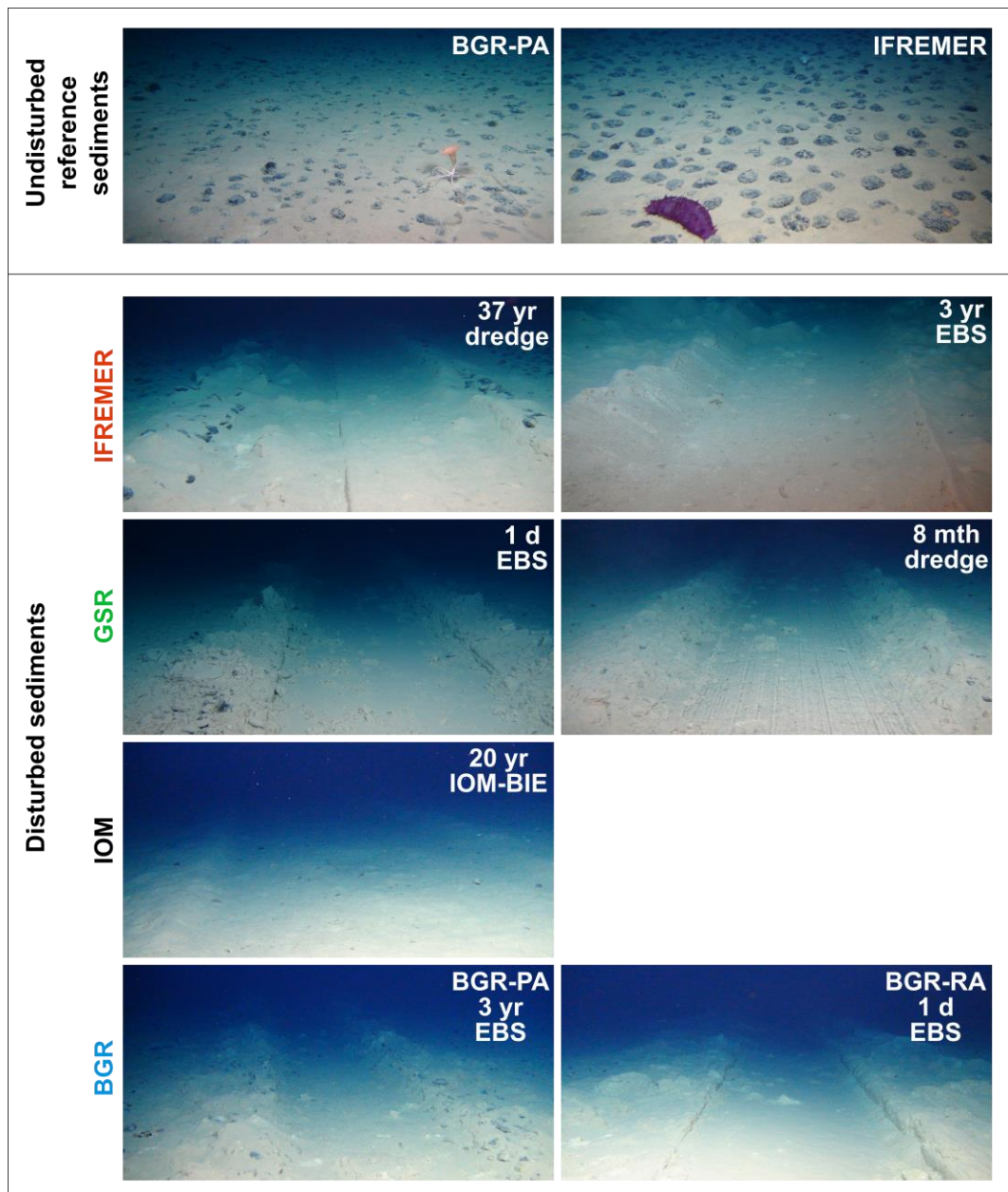
942 Table 3: Calculated Pearson correlation coefficients r_{Mn} and r_{TOC} for the determination of the
943 disturbance depth of various small-scale disturbances investigated in the framework of this
944 study (compare Table 1). For both correlations, the highest positive linear Pearson coefficient
945 for solid-phase Mn contents ($r_{\text{Mn}} \sim 1$) between the disturbed sites and the respective undisturbed
946 reference sites was used.

947

948 **Figure 1:**



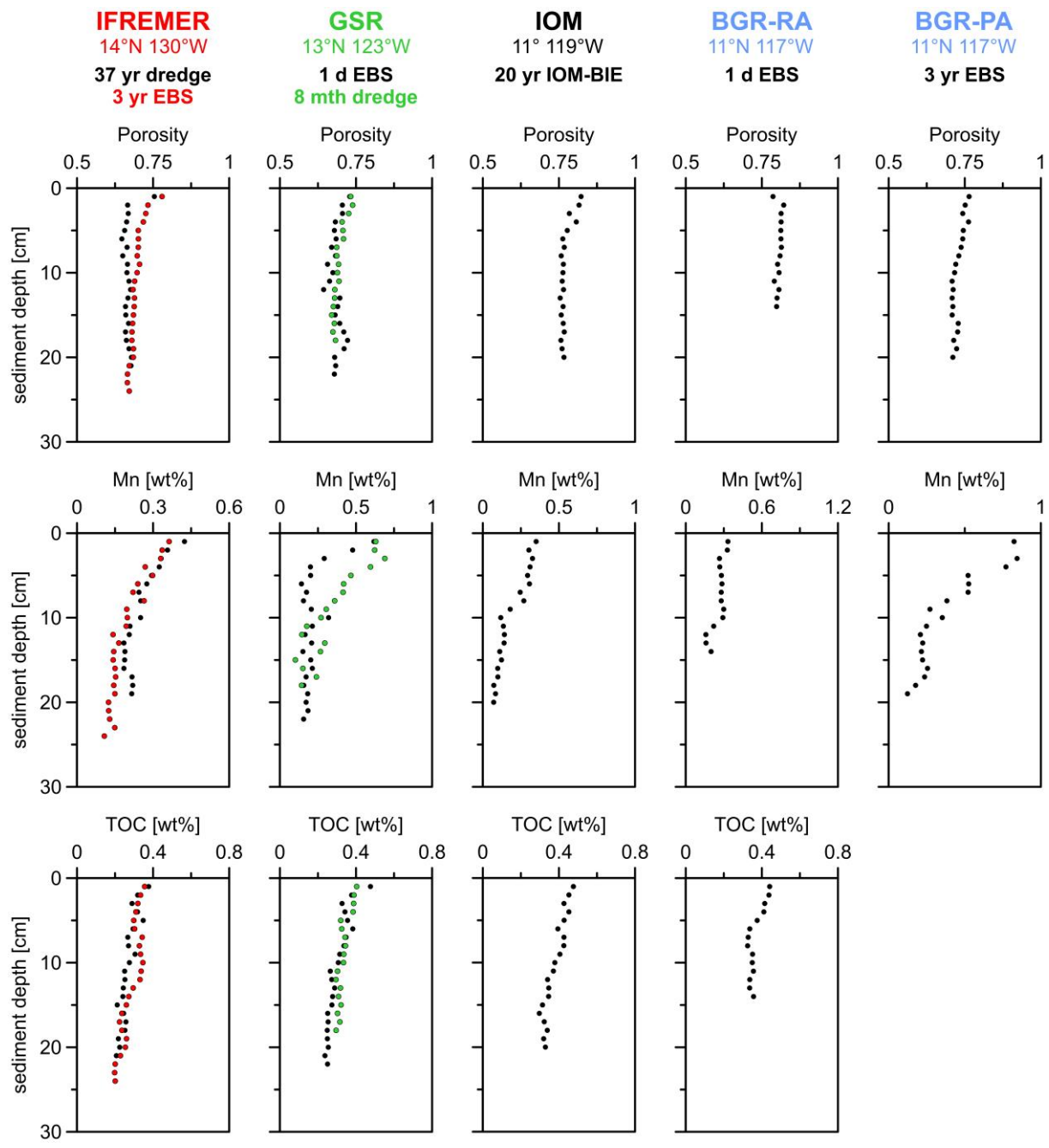
953 **Figure 2:**



954
955

956

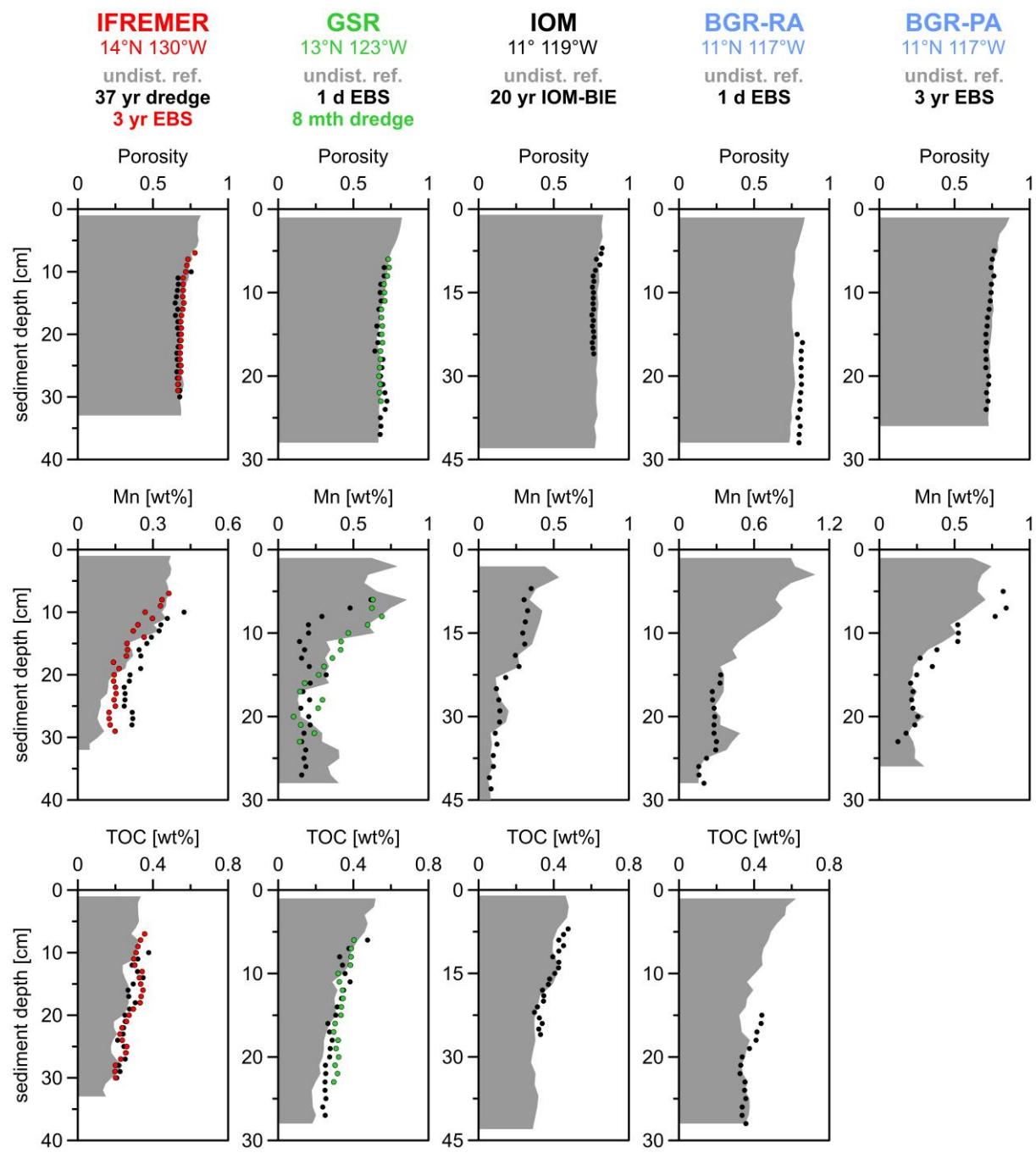
957 **Figure 3:**



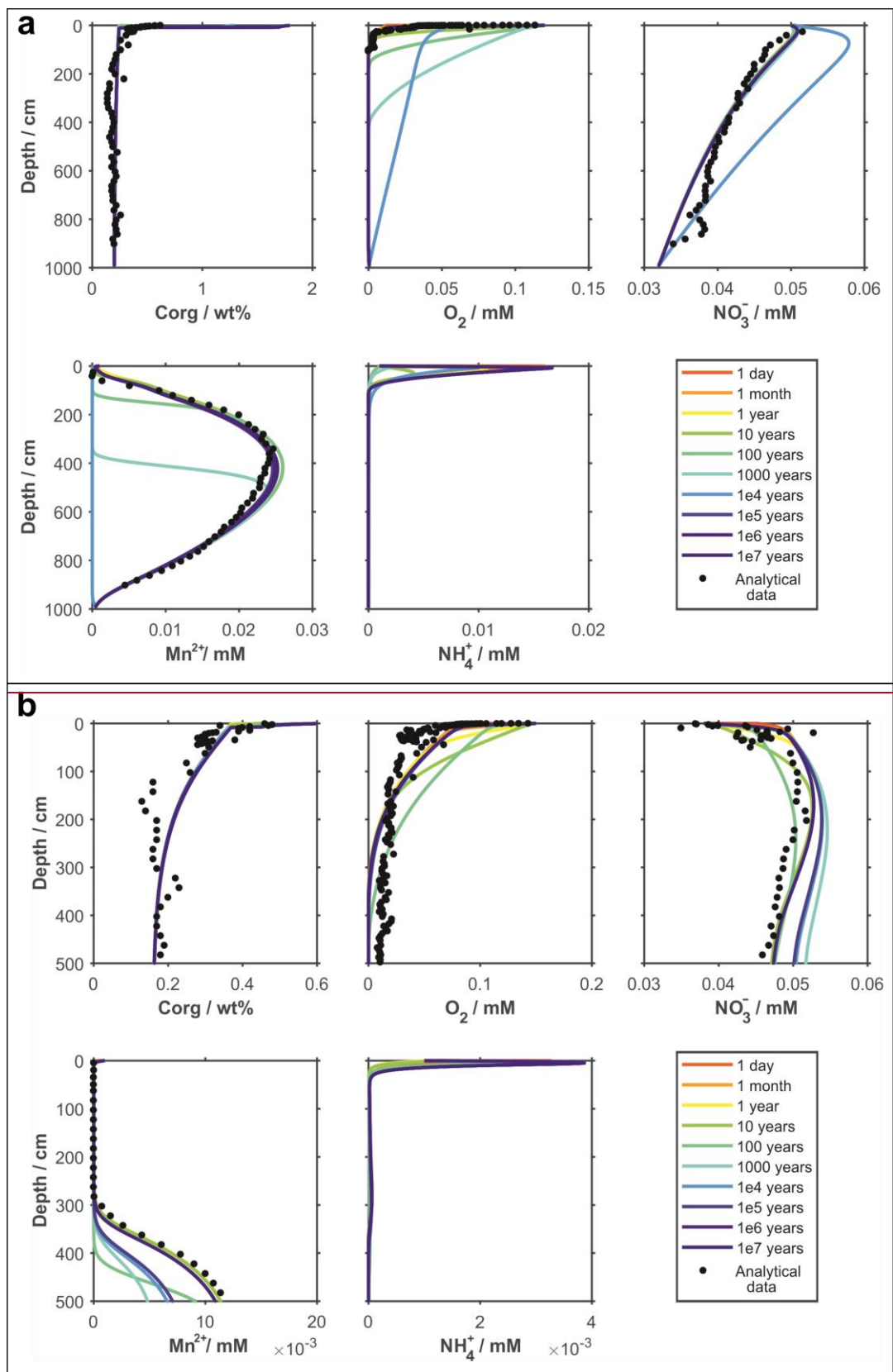
958

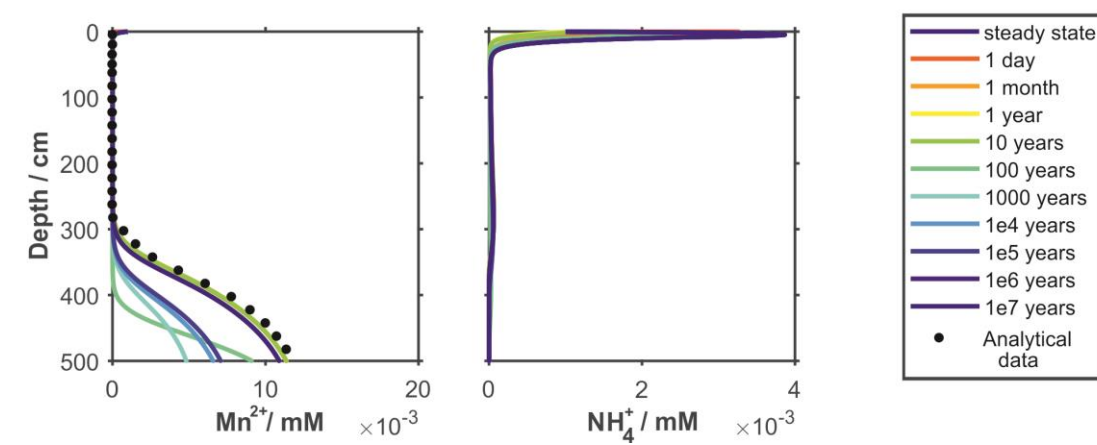
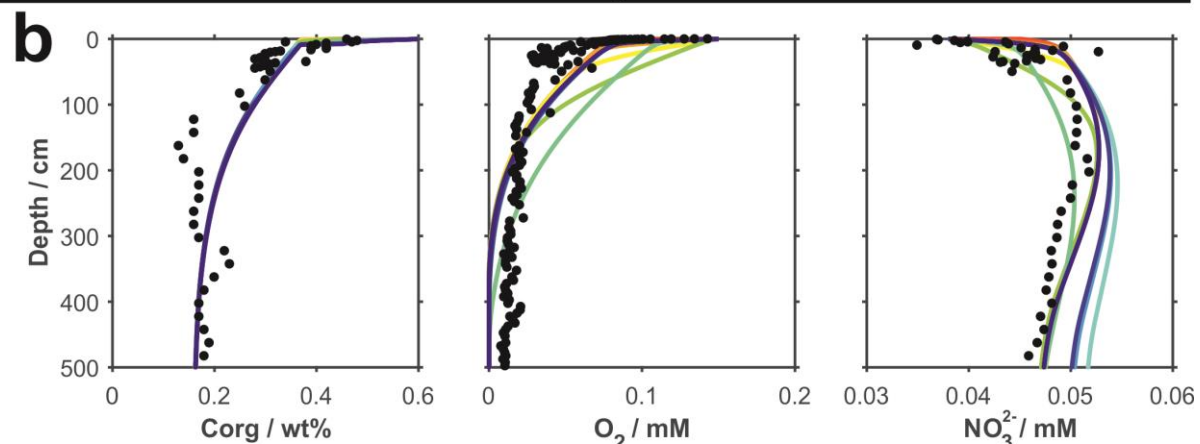
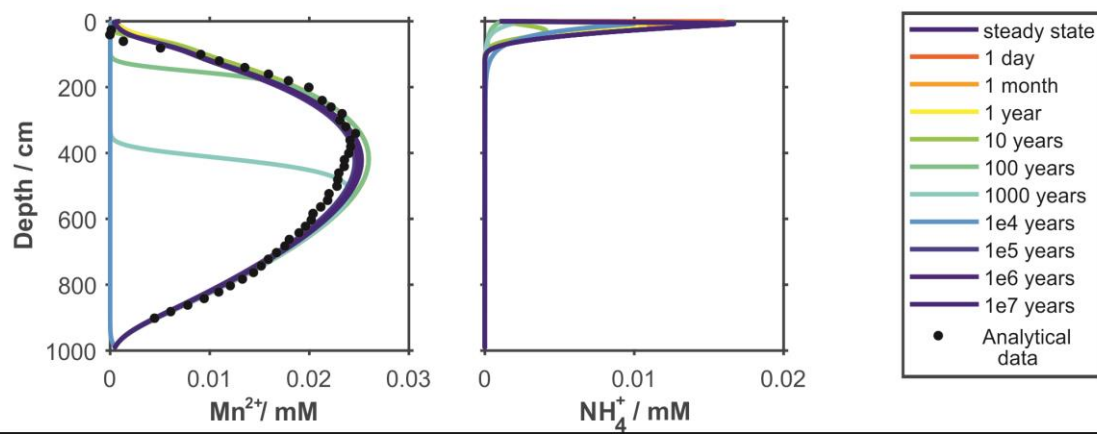
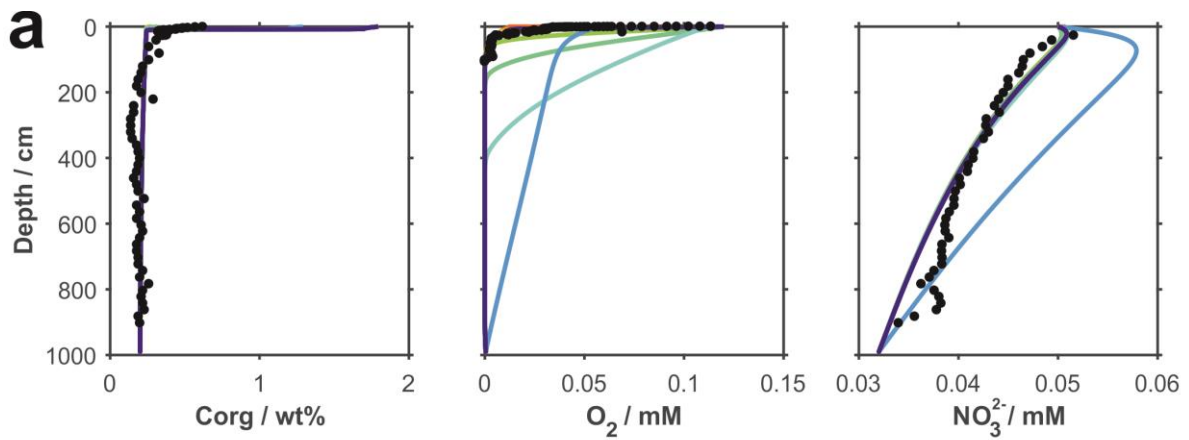
959

960 **Figure 4:**

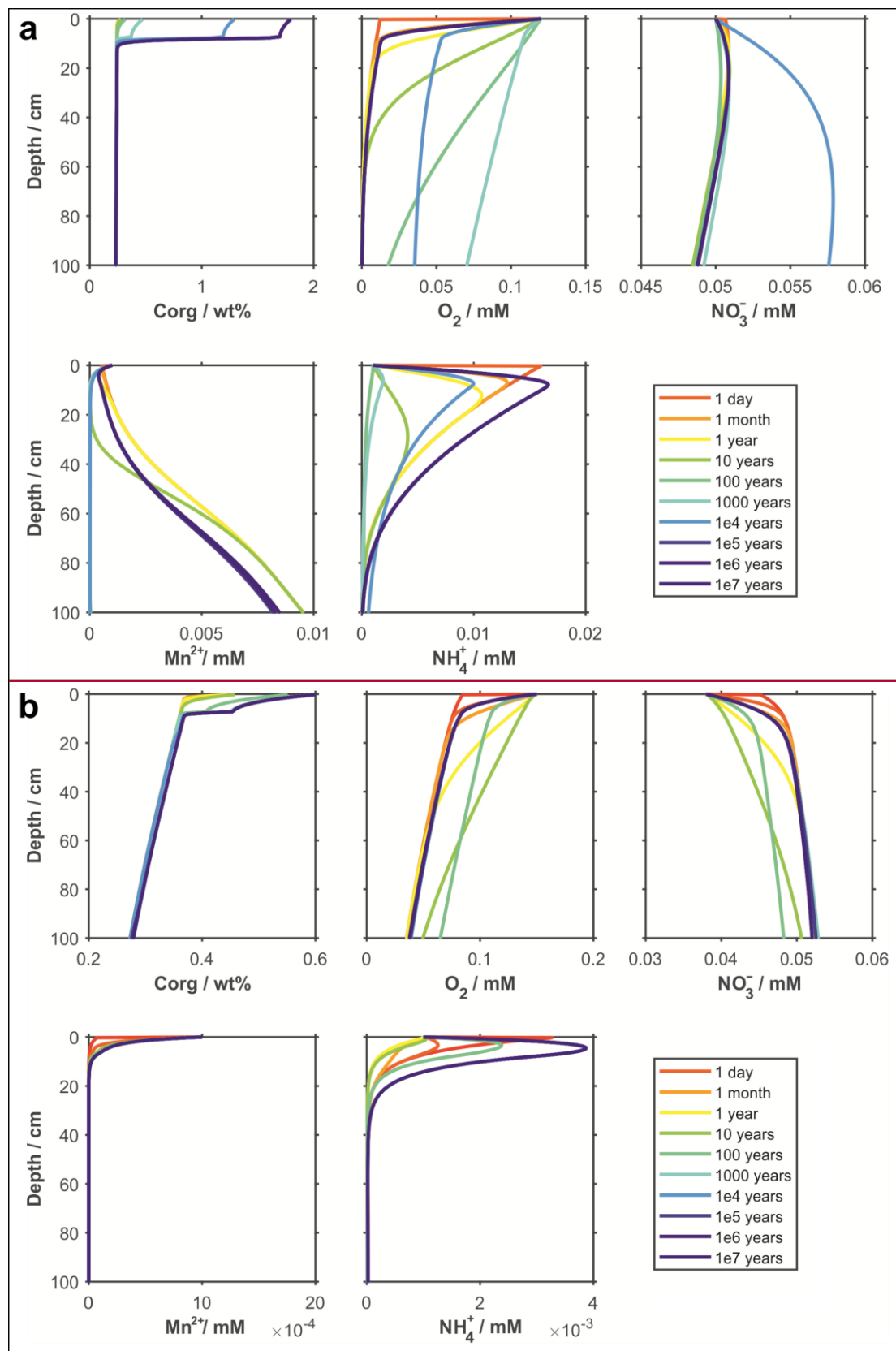


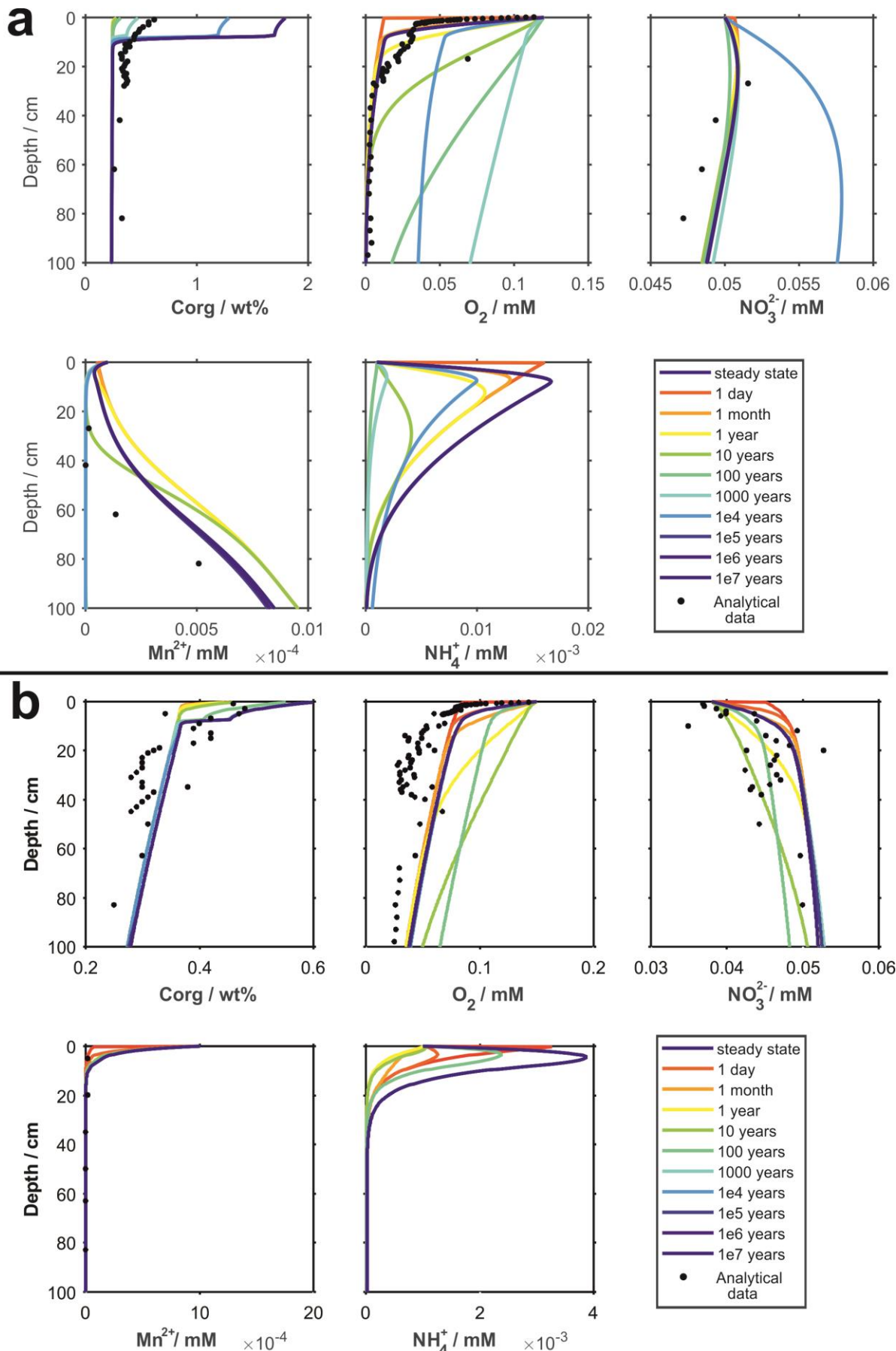
963 **Figure 5:**



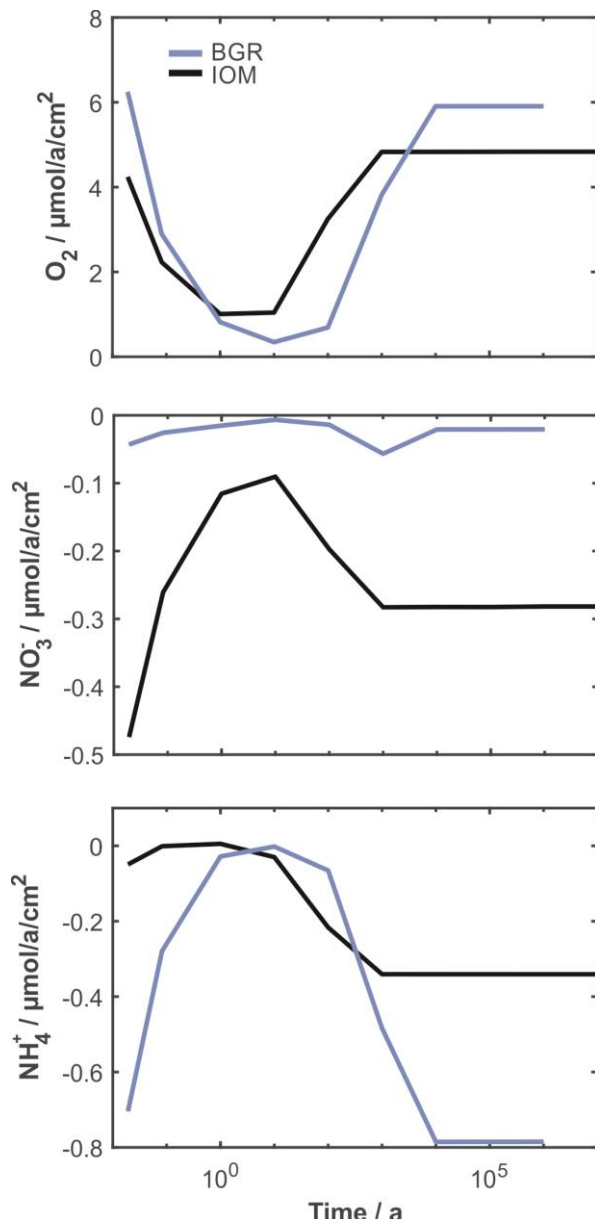


967 **Figure 6:**





971 **Figure 7:**

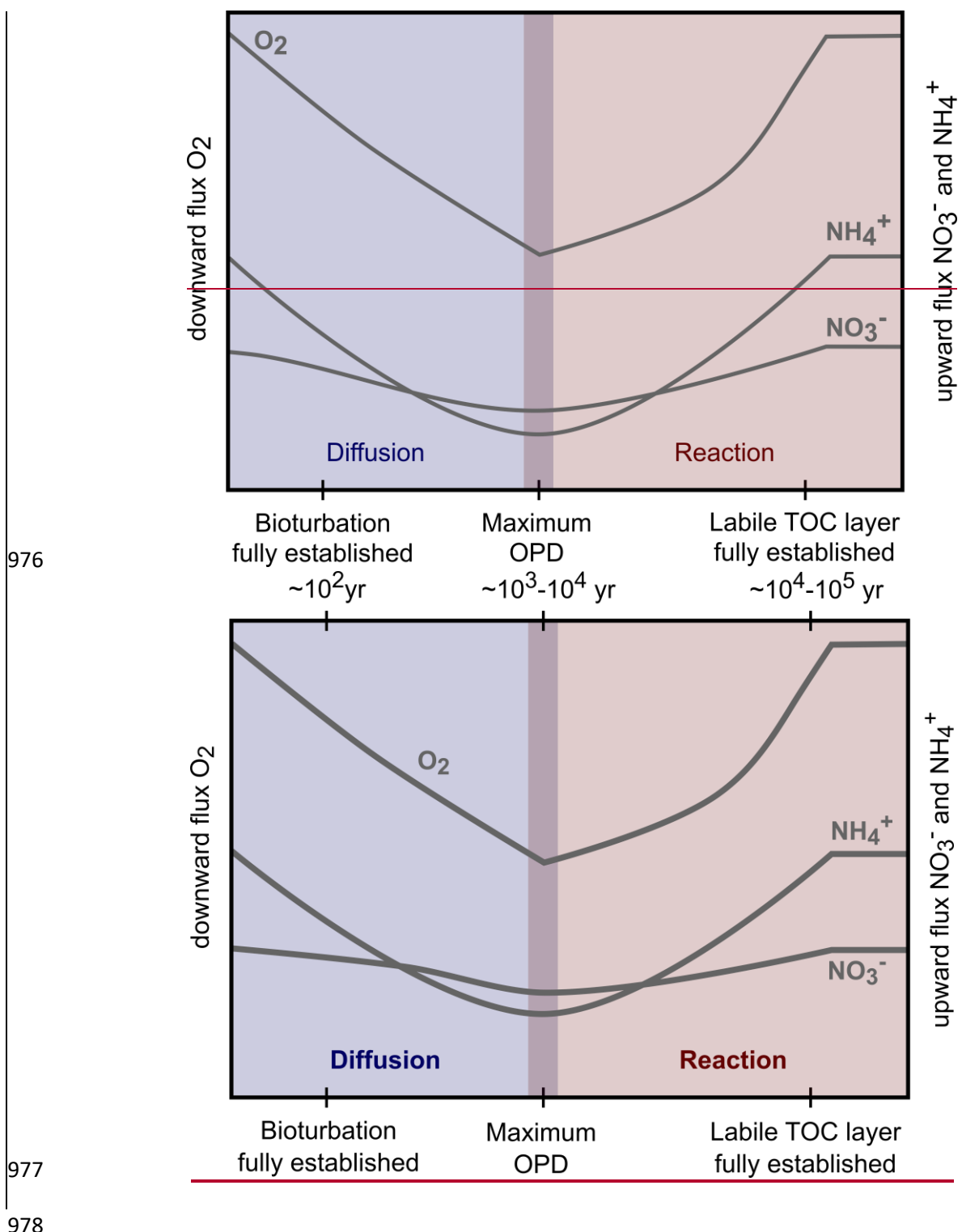


972

973

974

975 **Figure 8:**



979 **Table 1:**

Area	Site	Coring device	Disturbance device/type	Disturbance age	Latitude [N]	Longitude [W]	Water depth [m]
BGR-PA	39	MUC	-	-	11°50.64'	117°03.44'	4132.0
BGR-PA	41	PC	EBS ¹	3 yr	11°50.92'	117°03.77'	4099.2
BGR-RA	62	GC	-	-	11°49.12'	117°33.22'	4312.2
BGR-RA	64	PC	EBS ²	1 d	11°48.27'	117°30.18'	4332
BGR-RA	66	MUC	-	-	11°49.13'	117°33.13'	4314.8
IOM	84	MUC	-	-	11°04.73'	119°39.48'	4430.8
IOM	87	GC	-	-	11°04.54'	119°39.83'	4436
IOM	101	PC	IOM-BIE ³	20 yr	11°04.38'	119°39.38'	4387.4
GSR	121	MUC	-	-	13°51.25'	123°15.3'	4517.7
GSR	131	PC	EBS ²	1 d	13°52.38'	123°15.1'	4477.6
GSR	141	PC	dredge ⁴	8 mth	13°51.95'	123°15.33'	4477
IFREMER	157	PC	dredge ⁵	37 yr	14°02.06'	130°07.23'	4944.5
IFREMER	161	PC	EBS ¹	3 yr	14°02.20'	130°05.87'	4999.1
IFREMER	175	MUC	-	-	14°02.45'	130°05.11'	5005.5

980 ¹Epibenthic sledge (EBS) during BIONOD cruises in 2012 onboard L'Atalante (Brenke, 2005; Rühlemann and
981 Menot, 2012; Menot and Rühlemann, 2013)

982 ²Epibenthic sledge (EBS) during RV SONNE cruise SO239 in 2015 (Brenke, 2005; Martínez Arbizu and
983 Haeckel, 2015)

984 ³Benthic impact experiment (BIE); disturbance created with the Deep-Sea Sediment Re-suspension System
985 (DSSRS; e.g., Brocket and Richards, 1994; Kotlinski et al., 1998)

986 ⁴Towed dredge sampling during GSR cruise in 2014 onboard M.V. Mt Mitchell (Jones et al., 2017)

987 ⁵Towed dredge sampling by the Ocean Minerals Company (OMCO) in 1978 onboard Hughes Glomar Explorer
988 (Morgan et al., 1993; Spickermann, 2012)

990 **Table 2:**

Area	Sed. rate [cm kyr ⁻¹]	POC flux [mg C _{org} m ⁻² d ⁻¹]	Bioturb. depth [cm]	OPD [m]
BGR-PA	~0.53 ^a	~6.9 ^a	~5 ^a	~2 ^{a,b}
BGR-RA	0.65	1.99	7	0.5
IOM	1.15	1.54	13	3
GSR	0.21	1.51	8	>7.4
IFRE-1	0.64	1.47	7	4.5
IFRE-2	0.48	1.5	8	3.8
APEI3	0.2	1.07	6	>5.7

991 ^aMogollón et al. (2016)992 ^bMewes et al. (2014)

993

994

995 **Table 3:**

Exploration area	Disturbance device/type	Disturbed Site	Reference Site	r_{Mn}	Disturbance depth [cm]	r_{TOC}
BGR-PA	EBS	41	39	0.86	5	-
BGR-RA	EBS	64	66	0.82	15	-0.4
IOM	IOM-BIE	101	87	0.97	7	0.77
GSR	EBS	131	121	0.72	6	0.88
GSR	dredge	141	121	0.88	6	0.91
IFREMER	dredge	157	175	0.74	10	0.73
IFREMER	EBS	161	175	0.93	7	0.74

996

997